

PITHA 06/02
 IFIC/06-09
 ZU-TH 08/06
 UCLA/06/TEP/07

Two-Parton Contribution to the Heavy-Quark Forward-Backward Asymmetry in NNLO QCD

W. Bernreuther ^a, R. Bonciani ^b, T. Gehrmann ^c, R. Heinesch ^{a,1},
 T. Leineweber ^{a,2}, P. Mastrolia ^{c,d} and E. Remiddi ^e

^a *Institut für Theoretische Physik, RWTH Aachen, D-52056 Aachen, Germany*

^b *Departament de Física Teòrica, IFIC, CSIC – Universitat de València, E-46071 València, Spain*

^c *Institut für Theoretische Physik, Universität Zürich, CH-8057 Zürich, Switzerland*

^d *Department of Physics and Astronomy, UCLA, Los Angeles, CA 90090-1547, USA*

^e *Dipartimento di Fisica dell'Università di Bologna, and INFN, Sezione di Bologna, I-40126 Bologna, Italy*

Abstract

Forward-backward asymmetries, A_{FB}^Q , are important observables for the determination of the neutral-current couplings of heavy quarks in inclusive heavy quark production, $e^+e^- \rightarrow \gamma^*, Z^* \rightarrow Q + X$. In view of the measurement perspectives on A_{FB}^Q at a future linear collider, precise predictions of A_{FB}^Q are required for massive quarks. We compute the contribution of the $Q\bar{Q}$ final state to A_{FB}^Q to order α_s^2 in the QCD coupling. We provide general formulae, and we show that this contribution to A_{FB}^Q is infrared-finite. We evaluate these two-parton contributions for b and c quarks on and near the Z resonance, and for t quarks above threshold. Moreover, near the $t\bar{t}$ threshold we obtain, by expanding in the heavy-quark velocity β , an expression for $A_{FB}^{t\bar{t}}$ to order α_s^2 and NNLL in β . This quantity is equal, to this order in β , to the complete forward-backward asymmetry A_{FB}^t .

Key words: Electroweak measurements, Forward-backward asymmetry, Heavy quarks, Precision calculations, QCD corrections.

PACS: 12.38.Bx, 13.66.Jn, 14.65.Dw, 14.65.Fy, 14.65.Ha

¹present address: Framatome ANP GmbH, D-63067 Offenbach, Germany

²present address: Framatome ANP GmbH, D-91050 Erlangen, Germany

1 Introduction

Forward-backward asymmetries in the production of fermions in high-energy e^+e^- collisions are known to be precision observables for the determination of the respective fermionic neutral current couplings. Specifically the forward-backward asymmetry A_{FB}^b of b quarks, which was measured at the Z resonance with an accuracy of 1.7 percent, led to a determination of the effective weak mixing angle $\sin^2 \theta_{W,eff}$ of the Standard Model with a relative precision of about 1 per mille [1, 2] – notwithstanding the apparent discrepancy between this measurement and the determination of $\sin^2 \theta_{W,eff}$ with similar precision from the left-right asymmetry measured by the SLD collaboration. (For a comprehensive overview, see [1].)

At a future linear e^+e^- collider [3], precision determinations of electroweak parameters will again involve forward-backward asymmetries. When such a collider will be operated at the Z peak, accuracies of about 0.1 percent may be reached for these observables [4, 5]. Moreover, the top quark asymmetry A_{FB}^t will be experimentally accessible – a crucial tool for the determination of the hitherto unexplored neutral current couplings of this quark.

The theoretical understanding of these observables, in particular those involving the heavy quarks $Q = t, b, c$, must eventually match these projected accuracies. The present theoretical description of A_{FB}^b and A_{FB}^c includes the fully massive next-to-leading order (NLO) electroweak [6, 7, 8] and fully massive NLO QCD [9, 10, 11] corrections. The next-to-next-to-leading order (NNLO) QCD corrections, i.e., the contributions of α_s^2 to these asymmetries, were calculated so far only in the limit of massless quarks Q [12, 13, 14]. To be precise, the forward-backward asymmetry of *massless* quarks is not computable in QCD perturbation theory, as was pointed out in [14]. It is affected in the limit $m_Q \rightarrow 0$ by logarithmic final state divergences $\sim \ln m_Q$ resulting from the contribution of the $Q\bar{Q}Q\bar{Q}$ final state. (These terms are associated with the non-perturbative Q fragmentation function.) These logarithmically enhanced terms were taken into account in Ref. [14], which is the most complete calculation of A_{FB}^b within QCD to date, done both with respect to the quark and the thrust axis.

In view of the future perspectives for the b - and t -quark asymmetries at a linear collider, a computation of the order α_s^2 contributions to A_{FB}^Q for massive quarks Q is clearly desirable. The NNLO QCD corrections involve three classes of contributions: (1) the two-loop corrections to the decay of a vector boson into a heavy quark-antiquark pair; (2) the one-loop corrected matrix elements for the decay of a vector boson into a heavy quark-antiquark pair plus a gluon; (3) the tree level matrix elements for the decay of a vector boson into four partons, at least two of which being the heavy quark-antiquark pair.

In the limit of massless external quarks Q the $Q\bar{Q}$ contributions to A_{FB}^Q vanish up to a non-universal correction of order α_s^2 due to quark triangle diagrams [12]. This is no longer the case for $m_Q \neq 0$. In this paper we determine class (1), i.e., the order α_s^2 $Q\bar{Q}$ contributions to A_{FB}^Q , for arbitrary quark mass m_Q and center-of-mass (c.m.) energy \sqrt{s} . For this purpose we use our recent results on the two-loop vector and axial vector vertex functions for massive quarks [20, 21, 22] which determine the amplitude of $e^+e^- \rightarrow \gamma^*, Z^* \rightarrow Q\bar{Q}$ to order α_s^2 and to lowest order in the electroweak couplings. The contributions (1) from the two-parton final state, and (2) plus (3), i.e., those from the three- and four-parton final states, are separately infrared-finite, as will be discussed below. The latter can be obtained along the lines of the calculations of three-jet production involving heavy quarks [15, 16, 17]. The parity-violating part of $d\sigma(3jet)$ at order α_s^2 , which is a necessary ingredient here, was computed in [18].

However, a full computation of $A_{FB}^{3+4parton}$ has not yet been done for massive quarks.

The paper is organized as follows. In Section 2 we set up the formulae for determining A_{FB}^Q , off and at the Z resonance, to order α_s^2 in terms of the symmetric and antisymmetric cross sections for inclusive production of quarks Q . In particular we express the $Q\bar{Q}$ contribution to A_{FB}^Q by the one- and two-loop heavy-quark vector and axial vector form factors that determine the amplitude corresponding to the $Q\bar{Q}$ final state. Moreover, we show that these contributions to the respective forward-backward asymmetry, which we denote by $A_{FB}^{Q\bar{Q}}$, are infrared-finite. In Section 3 we present the NNLO $Q\bar{Q}$ cross section and the forward-backward asymmetry in the energy region $\alpha_s \ll \beta \ll 1$, where β denotes the heavy-quark velocity. This result is applicable, for instance, to t quarks in the vicinity of the $t\bar{t}$ threshold. In Section 4 we evaluate $A_{FB}^{Q\bar{Q}}$ for b and c quarks at the Z resonance, and in the case of t quarks for c. m. energies above the $t\bar{t}$ threshold till 1 TeV. We conclude in Section 5.

2 The Forward-Backward Asymmetry to Order α_s^2

In this paper we consider the production of a heavy quark-antiquark pair in e^+e^- collisions,

$$e^+e^- \rightarrow \gamma^*(q), Z^*(q) \rightarrow Q\bar{Q} + X, \quad (1)$$

where $Q = c, b, t$, to lowest order in the electroweak couplings and to second order in the QCD coupling α_s . To this order the following final states contribute to the cross section of inclusive $Q\bar{Q}$ production, Eq. (1): the two-parton $Q\bar{Q}$ state (at Born level, to order α_s , and to order α_s^2), the three-parton state $Q\bar{Q}g$ (to order α_s and to order α_s^2) and the four-parton states $Q\bar{Q}gg$, $Q\bar{Q}q\bar{q}$, and $Q\bar{Q}Q\bar{Q}$ (to order α_s^2).

The forward-backward asymmetry¹ A_{FB} for a heavy quark Q is commonly defined as the number of quarks Q observed in the forward hemisphere minus the number of quarks Q in the backward hemisphere, divided by the total number of observed quarks Q . The axis that defines the forward direction must be infrared- and collinear-safe in order that A_{FB} is computable in perturbation theory. Common choices are the direction of flight of Q or the thrust axis direction. The forward-backward asymmetry can also be expressed in terms of the cross section for inclusive production of quarks Q . We have:

$$A_{FB} = \frac{\sigma_A}{\sigma_S}, \quad (2)$$

with the antisymmetric and symmetric cross sections σ_A and $\sigma_S = \sigma$ defined by

$$\sigma_A = \int_0^1 \frac{d\sigma}{d\cos\vartheta} d\cos\vartheta - \int_{-1}^0 \frac{d\sigma}{d\cos\vartheta} d\cos\vartheta, \quad (3)$$

$$\sigma_S = \int_{-1}^1 \frac{d\sigma}{d\cos\vartheta} d\cos\vartheta. \quad (4)$$

Here ϑ is the angle between the incoming electron and the direction defining the forward hemisphere (in the e^+e^- center-of-mass frame). When choosing the momentum direction of Q

¹We drop the superscript Q in the following for ease of notation.

or the thrust axis, the $Q\bar{Q}$ contribution to A_{FB} , which we compute in this paper, is of course the same. In the following $\vartheta = \angle(e^-, Q)$.

In analogy to its experimental measurement, A_{FB} may be computed by determining the contributions from the final-state jets which, to order α_s^2 , are those of the two-, three-, and four-jet states. These contributions are separately infrared-finite, and A_{FB} would not depend on the jet clustering algorithm employed when no phase space cuts are applied. Such a calculation would require a jet calculus for massive quarks at NNLO in α_s which is, however, not available. (For massless quarks a NNLO subtraction method was recently developed [19], cf. also references therein.) Yet, A_{FB} belongs to the class of observables that can be computed at the level of unresolved partons. The two-parton and the three- plus four-parton contributions to the second-order forward-backward asymmetry are separately infrared (IR) finite, cf. [12, 14] and Section 2.2 below. This basic result will be exploited in the following.

To order α_s^2 the symmetric and antisymmetric cross sections receive the following contributions from unresolved partons:

$$\sigma_{A,S} = \sigma_{A,S}^{(2,0)} + \sigma_{A,S}^{(2,1)} + \sigma_{A,S}^{(2,2)} + \sigma_{A,S}^{(3,1)} + \sigma_{A,S}^{(3,2)} + \sigma_{A,S}^{(4,2)} + \mathcal{O}(\alpha_s^3), \quad (5)$$

where the first number in the superscripts (i, j) denotes the number of partons in the respective final state and the second one the order of α_s . Inserting (5) into (2) we get for A_{FB} to second order in α_s :

$$A_{\text{FB}}(\alpha_s^2) = \frac{\sigma_A^{(2,0)} + \sigma_A^{(2,1)} + \sigma_A^{(2,2)} + \sigma_A^{(3,1)} + \sigma_A^{(3,2)} + \sigma_A^{(4,2)}}{\sigma_S^{(2,0)} + \sigma_S^{(2,1)} + \sigma_S^{(2,2)} + \sigma_S^{(3,1)} + \sigma_S^{(3,2)} + \sigma_S^{(4,2)}}. \quad (6)$$

Taylor expansion of (6) with respect to α_s leads to

$$A_{\text{FB}}(\alpha_s^2) = A_{\text{FB},0} [1 + A_1 + A_2], \quad (7)$$

where $A_{\text{FB},0}$ is the forward-backward asymmetry at Born level, and A_1 and A_2 are the $\mathcal{O}(\alpha_s)$ and $\mathcal{O}(\alpha_s^2)$ contributions normalized to $A_{\text{FB},0}$.

$$A_{\text{FB},0} = \frac{\sigma_A^{(2,0)}}{\sigma_S^{(2,0)}}, \quad (8)$$

$$A_1 = \frac{\sigma_A^{(2,1)}}{\sigma_A^{(2,0)}} - \frac{\sigma_S^{(2,1)}}{\sigma_S^{(2,0)}} + \frac{\sigma_A^{(3,1)}}{\sigma_A^{(2,0)}} - \frac{\sigma_S^{(3,1)}}{\sigma_S^{(2,0)}}, \quad (9)$$

$$A_2 = \frac{\sigma_A^{(2,2)}}{\sigma_A^{(2,0)}} - \frac{\sigma_S^{(2,2)}}{\sigma_S^{(2,0)}} + \frac{\sigma_A^{(3,2)}}{\sigma_A^{(2,0)}} - \frac{\sigma_S^{(3,2)}}{\sigma_S^{(2,0)}} + \frac{\sigma_A^{(4,2)}}{\sigma_A^{(2,0)}} - \frac{\sigma_S^{(4,2)}}{\sigma_S^{(2,0)}} - \frac{\sigma_S^{(2,1)} + \sigma_S^{(3,1)}}{\sigma_S^{(2,0)}} \left[\frac{\sigma_A^{(2,1)}}{\sigma_A^{(2,0)}} - \frac{\sigma_S^{(2,1)}}{\sigma_S^{(2,0)}} + \frac{\sigma_A^{(3,1)}}{\sigma_A^{(2,0)}} - \frac{\sigma_S^{(3,1)}}{\sigma_S^{(2,0)}} \right]. \quad (10)$$

2.1 The $Q\bar{Q}$ Contribution

It is convenient to rewrite Eq. (7) as follows:

$$A_{\text{FB}}(\alpha_s^2) = A_{\text{FB}}^{(2p)} + A_{\text{FB}}^{(3p)} + A_{\text{FB}}^{(4p)}, \quad (11)$$

where the superscript (np) labels the number of partons n in the final state. Collecting the two-parton term from Eqs. (8), (9), and (10) we get:

$$A_{\text{FB}}^{(2p)} = A_{\text{FB},0} \left[1 + A_1^{(2p)} + A_2^{(2p)} \right], \quad (12)$$

with

$$A_1^{(2p)} = \frac{\sigma_A^{(2,1)}}{\sigma_A^{(2,0)}} - \frac{\sigma_S^{(2,1)}}{\sigma_S^{(2,0)}}, \quad (13)$$

$$A_2^{(2p)} = A_{2,2} - A_{2,1}, \quad (14)$$

where

$$A_{2,2} = \frac{\sigma_A^{(2,2)}}{\sigma_A^{(2,0)}} - \frac{\sigma_S^{(2,2)}}{\sigma_S^{(2,0)}}, \quad (15)$$

$$A_{2,1} = \frac{\sigma_S^{(2,1)}}{\sigma_S^{(2,0)}} A_1^{(2p)}. \quad (16)$$

The remaining terms in Eqs. (9), (10) contribute to $A^{(3p)}$ and $A^{(4p)}$.

As already stated above, both the two-parton and the three- plus four-parton contributions $A^{(2p)}$ and $A^{(3p)} + A^{(4p)}$, respectively, are infrared (IR) finite, i.e., free of soft and collinear singularities. We shall show this explicitly for $A^{(2p)}$ at the end of this section.

Next we express $A_{\text{FB}}^{(2p)}$ in terms of the $VQ\bar{Q}$ vertex form factors ($V = \gamma, Z$) which determine the amplitude of the reaction $e^+e^- \rightarrow \gamma^*, Z^* \rightarrow Q\bar{Q}$ to lowest order in the electroweak couplings and to any order in the QCD coupling; see Fig. 1. In this case the $VQ\bar{Q}$ vertex $\Gamma_Q^{\mu,V}$ depends,

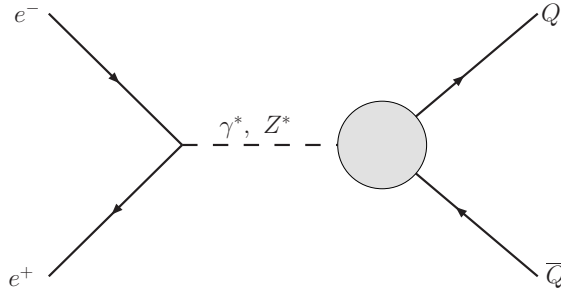


Figure 1: The amplitude $e^+e^- \rightarrow Q\bar{Q}$ in QCD.

for on-shell external quarks, on four form factors:

$$\begin{aligned} i \Gamma_Q^{\mu,V} &= v_Q^V \left(F_1(s) \gamma^\mu + \frac{i}{2m_Q} F_2(s) \sigma^{\mu\nu} q_\nu \right) \\ &+ a_Q^V \left(G_1(s) \gamma^\mu \gamma_5 + \frac{1}{2m_Q} G_2(s) \gamma_5 q^\mu \right), \end{aligned} \quad (17)$$

where $s = q^2$, $\sigma^{\mu\nu} = \frac{i}{2} [\gamma^\mu, \gamma^\nu]$, m_Q denotes the on-shell mass of Q , and, for $f = e, Q$,

$$\begin{aligned} v_f^Z &= \frac{e}{2s_W c_W} (T_f^3 - 2s_W^2 e_f) , \\ a_f^Z &= \frac{e}{2s_W c_W} (-T_f^3) , \\ v_f^\gamma &= e e_f , \quad a_f^\gamma = 0 . \end{aligned} \tag{18}$$

Here e_f and T_f^3 denote the charge of f in units of the positron charge e and its weak isospin, respectively, and s_W (c_W) are the sine (cosine) of the weak mixing angle θ_W . The functions F_i and G_i denote renormalized form factors; the renormalization scheme will be specified below. Instead of using the Dirac form factor F_1 we express in the following the (anti)symmetric cross section in terms of

$$\tilde{F}_1(s) = F_1(s) + F_2(s) . \tag{19}$$

Neglecting the electron mass we find for the two-parton contributions to $\sigma_{A,S}$:

$$\begin{aligned} \sigma_A^{(2p)} &= \frac{N_c}{8\pi} \frac{s}{D_Z} \beta^2 a_e^Z a_Q^Z \left\{ \left[v_e^Z v_Q^Z + \frac{1}{2} \left(1 - \frac{m_Z^2}{s} \right) v_e^\gamma v_Q^\gamma \right] \left(\tilde{F}_1^* G_1 + \tilde{F}_1 G_1^* \right) \right. \\ &\quad \left. + i \frac{m_Z \Gamma_Z}{2s} v_Q^\gamma v_e^\gamma \left(\tilde{F}_1 G_1^* - \tilde{F}_1^* G_1 \right) \right\} , \end{aligned} \tag{20}$$

$$\begin{aligned} \sigma_S^{(2p)} &= \frac{N_c}{24\pi} \frac{1}{s} \beta (v_e^\gamma v_Q^\gamma)^2 \mathcal{W} + \frac{N_c}{12\pi} \frac{s}{D_Z} \beta \left(1 - \frac{m_Z^2}{s} \right) v_e^\gamma v_Q^\gamma v_e^Z v_Q^Z \mathcal{W} \\ &\quad + \frac{N_c}{24\pi} \frac{s}{D_Z} \beta \left[(a_e^Z)^2 + (v_e^Z)^2 \right] \left[(v_Q^Z)^2 \mathcal{W} + 2\beta^2 (a_Q^Z)^2 (G_1 G_1^*) \right] , \end{aligned} \tag{21}$$

where

$$\mathcal{W} = (3 - \beta^2) \left(\tilde{F}_1 \tilde{F}_1^* \right) + \beta^2 \left(\tilde{F}_1 F_2^* + \tilde{F}_1^* F_2 \right) + \frac{\beta^4}{1 - \beta^2} (F_2 F_2^*) ,$$

$D_Z = [(s - m_Z^2)^2 + m_Z^2 \Gamma_Z^2]$ with m_Z , Γ_Z being the mass and width of the Z boson, $\beta = \sqrt{1 - \frac{4m_Q^2}{s}}$ the heavy quark velocity, and $N_c = 3$ the number of colors. Because we have put $m_e = 0$ the form factor G_2 does not contribute to Eqs. (20), (21). The last term in (20), which contains Γ_Z , is of higher order in the electroweak couplings as compared with the first term. We will neglect that term in the following.

Expanding the form factors in Eqs. (20), (21) in powers of α_s :

$$\tilde{F}_1 = 1 + \left(\frac{\alpha_s}{2\pi} \right) \tilde{F}_1^{(1\ell)} + \left(\frac{\alpha_s}{2\pi} \right)^2 \tilde{F}_1^{(2\ell)} + \mathcal{O}(\alpha_s^3) , \tag{22}$$

$$F_2 = \left(\frac{\alpha_s}{2\pi} \right) F_2^{(1\ell)} + \left(\frac{\alpha_s}{2\pi} \right)^2 F_2^{(2\ell)} + \mathcal{O}(\alpha_s^3) , \tag{23}$$

$$G_1 = 1 + \left(\frac{\alpha_s}{2\pi} \right) G_1^{(1\ell)} + \left(\frac{\alpha_s}{2\pi} \right)^2 G_1^{(2\ell)} + \mathcal{O}(\alpha_s^3) , \tag{24}$$

leads to the expansions of the two-parton contributions as exhibited in (5), i.e.,

$$\sigma_{A,S}^{(2p)} = \sigma_{A,S}^{(2,0)} + \sigma_{A,S}^{(2,1)} + \sigma_{A,S}^{(2,2)}. \quad (25)$$

The contributions to $\sigma_S^{(2p)}$ can be further decomposed as follows:

$$\sigma_S^{(2,0)} = \sigma_S^{(2,0,\gamma)} + \sigma_S^{(2,0,Z)} + \sigma_S^{(2,0,\gamma Z)}, \quad (26)$$

$$\sigma_S^{(2,1)} = \sigma_S^{(2,0,\gamma)} \sigma_S^{(2,1,\gamma)} + \sigma_S^{(2,0,Z)} \sigma_S^{(2,1,Z)} + \sigma_S^{(2,0,\gamma Z)} \sigma_S^{(2,1,\gamma Z)}, \quad (27)$$

$$\sigma_S^{(2,2)} = \sigma_S^{(2,0,\gamma)} \sigma_S^{(2,2,\gamma)} + \sigma_S^{(2,0,Z)} \sigma_S^{(2,2,Z)} + \sigma_S^{(2,0,\gamma Z)} \sigma_S^{(2,2,\gamma Z)}, \quad (28)$$

where the superscripts γ , Z , and γZ label the pure photon and Z contributions, and the $\gamma - Z$ interference terms, respectively. These terms are given by

$$\sigma_S^{(2,0,\gamma)} = \frac{N_c}{24\pi} \frac{1}{s} \beta (v_e^\gamma v_Q^\gamma)^2 (3 - \beta^2), \quad (29)$$

$$\sigma_S^{(2,1,\gamma)} = \left(\frac{\alpha_s}{2\pi} \right) \left\{ 2\text{Re} \tilde{F}_1^{(1\ell)} + \frac{2\beta^2}{3 - \beta^2} \text{Re} F_2^{(1\ell)} \right\}, \quad (30)$$

$$\begin{aligned} \sigma_S^{(2,2,\gamma)} &= \left(\frac{\alpha_s}{2\pi} \right)^2 \left\{ \frac{2\beta^2}{3 - \beta^2} \left[\text{Re} F_2^{(2\ell)} + \text{Re} \tilde{F}_1^{(1\ell)} \text{Re} F_2^{(1\ell)} + \pi^2 \text{Im} \tilde{F}_1^{(1\ell)} \text{Im} F_2^{(1\ell)} \right] \right. \\ &\quad \left. + \frac{\beta^4}{(3 - \beta^2)(1 - \beta^2)} \left[(\text{Re} F_2^{(1\ell)})^2 + \pi^2 (\text{Im} F_2^{(1\ell)})^2 \right] \right. \\ &\quad \left. + (\text{Re} \tilde{F}_1^{(1\ell)})^2 + \pi^2 (\text{Im} \tilde{F}_1^{(1\ell)})^2 + 2\text{Re} \tilde{F}_1^{(2\ell)} \right\}, \end{aligned} \quad (31)$$

$$\sigma_S^{(2,0,Z)} = \frac{N_c}{24\pi} \frac{s}{D_Z} \beta \left[(a_e^Z)^2 + (v_e^Z)^2 \right] \left[2(a_Q^Z)^2 \beta^2 + (v_Q^Z)^2 (3 - \beta^2) \right], \quad (32)$$

$$\sigma_S^{(2,1,Z)} = \frac{(v_Q^Z)^2 (3 - \beta^2) \sigma_S^{(2,1,\gamma)} + 4 \left(\frac{\alpha_s}{2\pi} \right) (a_Q^Z)^2 \beta^2 \text{Re} G_1^{(1\ell)}}{2(a_Q^Z)^2 \beta^2 + (3 - \beta^2) (v_Q^Z)^2}, \quad (33)$$

$$\begin{aligned} \sigma_S^{(2,2,Z)} &= \frac{1}{2(a_Q^Z)^2 \beta^2 + (3 - \beta^2) (v_Q^Z)^2} \left\{ (v_Q^Z)^2 (3 - \beta^2) \sigma_S^{(2,2,\gamma)} \right. \\ &\quad \left. + 4 \left(\frac{\alpha_s}{2\pi} \right)^2 (a_Q^Z)^2 \beta^2 \text{Re} G_1^{(2\ell)} + 2 \left(\frac{\alpha_s}{2\pi} \right)^2 (a_Q^Z)^2 \beta^2 \left[(\text{Re} G_1^{(1\ell)})^2 + \pi^2 (\text{Im} G_1^{(1\ell)})^2 \right] \right\}, \end{aligned} \quad (34)$$

$$\sigma_S^{(2,0,\gamma Z)} = \frac{N_c}{12\pi} \frac{s}{D_Z} \beta \left(1 - \frac{m_Z^2}{s} \right) v_e^\gamma v_Q^\gamma v_e^Z v_Q^Z (3 - \beta^2), \quad (35)$$

$$\sigma_S^{(2,1,\gamma Z)} = \sigma_S^{(2,1,\gamma)}, \quad (36)$$

$$\sigma_S^{(2,2,\gamma Z)} = \sigma_S^{(2,2,\gamma)}, \quad (37)$$

where the convention $F_a = \text{Re} F_a + i\pi \text{Im} F_a$, $G_a = \text{Re} G_a + i\pi \text{Im} G_a$ ($a = 1, 2$) is used; i.e., a

factor π is taken out of the imaginary part. The antisymmetric cross section is given by:

$$\sigma_A^{(2,0)} = \frac{N_c}{4\pi} \frac{s}{D_Z} \beta^2 a_e^Z a_Q^Z \left[v_e^Z v_Q^Z + \frac{1}{2} \left(1 - \frac{m_Z^2}{s} \right) v_e^\gamma v_Q^\gamma \right], \quad (38)$$

$$\sigma_A^{(2,1)} = \sigma_A^{(2,0)} \left(\frac{\alpha_s}{2\pi} \right) \left[\text{Re} \tilde{F}_1^{(1\ell)} + \text{Re} G_1^{(1\ell)} \right], \quad (39)$$

$$\sigma_A^{(2,2)} = \sigma_A^{(2,0)} \left(\frac{\alpha_s}{2\pi} \right)^2 \left[\text{Re} \tilde{F}_1^{(2\ell)} + \text{Re} G_1^{(2\ell)} + \text{Re} \tilde{F}_1^{(1\ell)} \text{Re} G_1^{(1\ell)} + \pi^2 \text{Im} \tilde{F}_1^{(1\ell)} \text{Im} G_1^{(1\ell)} \right]. \quad (40)$$

With these formulæ the $Q\bar{Q}$ contribution (12) to the forward-backward asymmetry is expressed in terms of the one- and two-loop form factors Eqs. (22) - (24).

The second order term in the expansion (24) of the axial vector form factor, $G_1^{(2\ell)}$, receives so-called type A and type B contributions. Type A contributions are those where the Z boson couples directly to the external quark Q [21], while the triangle diagram contributions, summed over the quark isodoublets of the three generations, are called type B [22]. (In the terminology of [14] these correspond to universal and non-universal corrections, respectively.) Among Eqs. (29) - (40) only $\sigma_S^{(2,2,Z)}$ and $\sigma_A^{(2,2)}$ depend on $G_1^{(2\ell)}$. With $G_1^{(2\ell)} = G_1^{(2\ell,A)} + G_1^{(2\ell,B)}$ we separate in these terms the type A and B contributions:

$$\sigma_S^{(2,2,Z)} = \sigma_S^{(2,2,Z,A)} + \sigma_S^{(2,2,Z,B)} \quad (41)$$

with

$$\sigma_S^{(2,2,Z,A)} = \sigma_S^{(2,2,Z)}(G_1^{(2\ell)} \rightarrow G_1^{(2\ell,A)}), \quad (42)$$

$$\sigma_S^{(2,2,Z,B)} = \left(\frac{\alpha_s}{2\pi} \right)^2 \frac{4 (a_Q^Z)^2 \beta^2 \text{Re} G_1^{(2\ell,B)}}{2 (a_Q^Z)^2 \beta^2 + (3 - \beta^2) (v_Q^Z)^2}, \quad (43)$$

and

$$\sigma_A^{(2,2)} = \sigma_A^{(2,2,A)} + \sigma_A^{(2,2,B)} \quad (44)$$

with

$$\sigma_A^{(2,2,A)} = \sigma_A^{(2,2)}(G_1^{(2\ell)} \rightarrow G_1^{(2\ell,A)}), \quad (45)$$

$$\sigma_A^{(2,2,B)} = \left(\frac{\alpha_s}{2\pi} \right)^2 \sigma_A^{(2,0)} \text{Re} G_1^{(2\ell,B)}. \quad (46)$$

Thus (14) can be written:

$$A_2^{(2p)} = A_2^{(2p,A)} + A_2^{(2p,B)}, \quad (47)$$

where $A_2^{(2p,A)}$ is obtained from (14) by the substitution $G_1^{(2\ell)} \rightarrow G_1^{(2\ell,A)}$ in (14), respectively in (15), and

$$A_2^{(2p,B)} = \frac{\sigma_A^{(2,2,B)}}{\sigma_A^{(2,0)}} - \frac{\sigma_S^{(2,0,Z)} \sigma_S^{(2,2,Z,B)}}{\sigma_S^{(2,0)}}. \quad (48)$$

If one evaluates, in the case of $b\bar{b}$ and $c\bar{c}$ final states, Eq. (48) exactly at the Z resonance and neglects the contributions from photon exchange, then:

$$A_2^{(2p,B)}(s = m_Z^2) = \left(\frac{\alpha_s}{2\pi}\right)^2 \operatorname{Re} G_1^{(2\ell,B)} \left[\frac{(3 - \beta^2) (v_Q^Z)^2 - 2 (a_Q^Z)^2 \beta^2}{(3 - \beta^2) (v_Q^Z)^2 + 2 (a_Q^Z)^2 \beta^2} \right]. \quad (49)$$

The type B contribution (48) to the forward-backward asymmetry is ultraviolet- and infrared-finite [22].

2.2 Infrared-Finiteness of $A_{\text{FB}}^{(2p)}$

The renormalized vector and axial vector form factors (17) were computed in [20, 21, 22] to order α_s^2 within QCD with N_f massless and one massive quark Q , in a renormalization scheme, which is appropriate for the case at hand: the wavefunction and the mass of Q are defined in the on-shell scheme while α_s is defined in the $\overline{\text{MS}}$ scheme. The renormalized form factors still contain IR divergences which are regulated by dimensional regularization in $D = 4 - 2\epsilon$ dimensions. At one loop, $F_1^{(1\ell)}$ and $G_1^{(1\ell)}$ contain $1/\epsilon$ poles due to soft virtual gluons. At two loops, the dominant IR singularities of $F_1^{(2\ell)}$ and $G_1^{(2\ell,A)}$ are of order $1/\epsilon^2$ due to soft and collinear massless partons, while $F_2^{(2\ell)}$ has only $1/\epsilon$ poles. However, when inserting the renormalized form factors into the formulae for the order α_s and α_s^2 contributions to $A_{\text{FB}}^{(2p)}$ the IR singularities cancel and we obtain a finite result. This is well-known for $A_1^{(2p)}$, c.f. [11].

This cancellation of infrared poles can be seen in a straightforward manner if one takes into account the universal structure of the infrared poles in the form factors, which can be expressed in terms of one-loop and two-loop infrared singularity operators for a massive quark-antiquark pair, $I_{Q\bar{Q}}^{(1)}(s, \mu = m_Q, \epsilon)$ and $I_{Q\bar{Q}}^{(2)}(s, \mu = m_Q, \epsilon)$, where μ is the renormalization scale, as:

$$\begin{aligned} \text{Poles} \left(F_1^{(1\ell)} \right) &= I_{Q\bar{Q}}^{(1)} F_1^{(0\ell)}, \\ \text{Poles} \left(F_2^{(1\ell)} \right) &= 0, \\ \text{Poles} \left(G_1^{(1\ell)} \right) &= I_{Q\bar{Q}}^{(1)} G_1^{(0\ell)}, \end{aligned} \quad (50)$$

$$\begin{aligned} \text{Poles} \left(F_1^{(2\ell)} \right) &= I_{Q\bar{Q}}^{(2)} F_1^{(0\ell)} + I_{Q\bar{Q}}^{(1)} F_1^{(1\ell)}, \\ \text{Poles} \left(F_2^{(2\ell)} \right) &= I_{Q\bar{Q}}^{(1)} F_2^{(1\ell)}, \\ \text{Poles} \left(G_1^{(2\ell)} \right) &= I_{Q\bar{Q}}^{(2)} G_1^{(0\ell)} + I_{Q\bar{Q}}^{(1)} G_1^{(1\ell)}. \end{aligned} \quad (51)$$

This factorization of the infrared poles is a well-known feature of massless multi-loop amplitudes, where it can be derived from exponentiation [23, 24]. In massive QED, the same behaviour was observed long ago [25]. To the best of our knowledge, infrared factorization in massive QCD was established up to now only at the one-loop level [26]; the above pole structure of the form factors suggests that it holds at higher orders as well. Expressions for $I_{Q\bar{Q}}^{(1,2)}$ can be read off from the explicit pole structure of the form factors [20, 21]. Exploiting that

$$F_1^{(0\ell)} = G_1^{(0\ell)} = 1,$$

one finds immediately that the two-parton contribution (14) to the forward-backward asymmetry is infrared finite. However, it should be kept in mind that the two terms in (14) are not separately finite.

Let us illustrate how this cancellation occurs in $A_2^{(2p)}$ by considering this expression at the Z resonance, i.e., by taking into account only Z exchange contributions and neglecting the photon and $\gamma - Z$ interference terms. When inserting the form factors into Eq. (15), all the leading $1/\epsilon^2$ singularities cancel, but a subleading divergence remains:

$$A_{2,2} = - \left(\frac{\alpha_s}{2\pi} \right)^2 C_F^2 \frac{1}{\epsilon} 4y \frac{2(a_Q^Z)^2(1-y)^2 - 3(v_Q^Z)^2(1+y)^2}{[(a_Q^Z)^2(1-y)^2 + (v_Q^Z)^2(1+y)^2 + 2(v_Q^Z)^2y] (1-y^2)^2} \times [(1+y^2) \ln^2(y) + (1-y^2) \ln(y)] + A_{2,2}^{finite} \quad (52)$$

where $y = (1 - \beta)/(1 + \beta)$ and $C_F = (N_c^2 - 1)/(2N_c)$. This subleading singularity proportional to C_F^2 results from the real parts of the one-loop form factors, $F_1^{(1\ell)}$ and $G_1^{(1\ell)}$, and from the contribution of a set of abelian-type two-loop diagrams (gluon ladder diagram and gluon vertex diagrams with quark self-energy insertions) to the real parts of the two-loop vector and type A axial vector form factors. The singularity (52) is removed by the second term in (14). While

$$A_1^{(2p)} = \frac{\alpha_s}{2\pi} C_F \ln(y) 2y \frac{2(a_Q^Z)^2(1-y)^2 - 3(v_Q^Z)^2(1+y)^2}{[(a_Q^Z)^2(1-y)^2 + (v_Q^Z)^2(1+y)^2 + 2(v_Q^Z)^2y] (1-y^2)} \quad (53)$$

is finite, the first term in (16) contains a singularity,

$$\frac{\sigma_S^{(2,1)}}{\sigma_S^{(2,0)}} = - \frac{\alpha_s}{2\pi} C_F \frac{1}{\epsilon} \frac{2(1-y^2 + (1+y)^2 \ln(y))}{1-y^2} + \text{finite terms}, \quad (54)$$

and thus the singular part of $A_{2,1}$ cancels the singularity in (52). This cancellation pattern remains also away from the Z resonance.

3 Cross Section and A_{FB} near Threshold

In this section we analyze the cross section and $A_{\text{FB}}^{(2p)}$ for $e^+e^- \rightarrow \gamma^*, Z^* \rightarrow Q\bar{Q}$ near the production threshold. Close to threshold, where the quark velocity β is small, the fixed order perturbative expansion in α_s of these and other quantities breaks down due to Coulomb singularities, which must be resummed. In addition, large logarithms in β appear, which may be summed using the renormalization group [27, 28] applied in the framework of nonrelativistic effective field theory methods. However, in the energy region where $\alpha_s \ll \beta \ll 1$, threshold expansions of observables, i.e., expansions in β to fixed order in α_s are expected to yield reliable results. In this region we derive compact formulae for the symmetric and antisymmetric $Q\bar{Q}$ cross sections at NNLO. These expressions should be useful, especially in the case of top-quark pair production, for comparison of continuum results with results obtained directly at threshold.

3.1 The $Q\bar{Q}$ cross section

We start with Eqs. (25) - (28) where the $Q\bar{Q}$ cross section at NNLO, $\sigma_{\text{NNLO}} = \sigma_S^{(2p)}$, is expressed in terms of the γ , Z , and $\gamma - Z$ exchange contributions. Using these formulae we

may write

$$\sigma_{NNLO} = \sigma_S^{(2,0,\gamma)} \left\{ 1 + \frac{\sigma_S^{(2,0,Z)} + \sigma_S^{(2,0,\gamma Z)}}{\sigma_S^{(2,0,\gamma)}} + \sigma_S^{(2,1,\gamma)} \left[1 + \frac{\sigma_S^{(2,0,Z)} \sigma_S^{(2,1,Z)} + \sigma_S^{(2,0,\gamma Z)} \sigma_S^{(2,1,\gamma Z)}}{\sigma_S^{(2,0,\gamma)} \sigma_S^{(2,1,\gamma)}} \right] \right. \\ \left. + \sigma_S^{(2,2,\gamma)} \left[1 + \frac{\sigma_S^{(2,0,Z)} \sigma_S^{(2,2,Z)} + \sigma_S^{(2,0,\gamma Z)} \sigma_S^{(2,2,\gamma Z)}}{\sigma_S^{(2,0,\gamma)} \sigma_S^{(2,2,\gamma)}} \right] \right\}. \quad (55)$$

Denoting

$$\Delta^{(0,Ax)} = \frac{\sigma_S^{(2,0,Z)} + \sigma_S^{(2,0,\gamma Z)}}{\sigma_S^{(2,0,\gamma)}} \quad (56)$$

and recalling Eqs. (36), (37) we get

$$\sigma_{NNLO} = \sigma_S^{(2,0,\gamma)} \left\{ 1 + \Delta^{(0,Ax)} + \sigma_S^{(2,1,\gamma)} \left[1 + \Delta^{(0,Ax)} \right] + \frac{\sigma_S^{(2,0,Z)}}{\sigma_S^{(2,0,\gamma)}} \left(\sigma_S^{(2,1,Z)} - \sigma_S^{(2,1,\gamma)} \right) \right. \\ \left. + \sigma_S^{(2,2,\gamma)} \left[1 + \Delta^{(0,Ax)} \right] + \frac{\sigma_S^{(2,0,Z)}}{\sigma_S^{(2,0,\gamma)}} \left(\sigma_S^{(2,2,Z)} - \sigma_S^{(2,2,\gamma)} \right) \right\}. \quad (57)$$

Putting

$$\frac{\sigma_S^{(2,0,Z)}}{\sigma_S^{(2,0,\gamma)}} \left(\sigma_S^{(2,1,Z)} - \sigma_S^{(2,1,\gamma)} \right) = C_F \left(\frac{\alpha_s}{2\pi} \right) \Delta^{(1,Ax)}, \quad (58)$$

$$\frac{\sigma_S^{(2,0,Z)}}{\sigma_S^{(2,0,\gamma)}} \left(\sigma_S^{(2,2,Z)} - \sigma_S^{(2,2,\gamma)} \right) = C_F \left(\frac{\alpha_s}{2\pi} \right)^2 \Delta^{(2,Ax)}, \quad (59)$$

the NNLO cross section reads:

$$\sigma_{NNLO} = \sigma_S^{(2,0,\gamma)} \left\{ 1 + \Delta^{(0,Ax)} + \sigma_S^{(2,1,\gamma)} \left[1 + \Delta^{(0,Ax)} \right] + C_F \left(\frac{\alpha_s}{2\pi} \right) \Delta^{(1,Ax)} \right. \\ \left. + \sigma_S^{(2,2,\gamma)} \left[1 + \Delta^{(0,Ax)} \right] + C_F \left(\frac{\alpha_s}{2\pi} \right)^2 \Delta^{(2,Ax)} \right\}. \quad (60)$$

We now expand the expression in the curly brackets of Eq. (60) up to and including terms of order β^0 . Using the threshold expansions [20, 21, 22] of the one- and two-loop vector and axial vector form factors and putting the renormalization scale $\mu = m_Q$ we obtain

$$\sigma_{NNLO} = \sigma_S^{(2,0,\gamma)} \left\{ 1 + \Delta^{(0,Ax)} + C_F \left(\frac{\alpha_s}{2\pi} \right) \Delta^{(1,Ve)} (1 + \Delta^{(0,Ax)}) + C_F \left(\frac{\alpha_s}{2\pi} \right) \Delta^{(1,Ax)} \right. \\ \left. + C_F \left(\frac{\alpha_s}{2\pi} \right)^2 \Delta^{(2,Ve)} (1 + \Delta^{(0,Ax)}) + C_F \left(\frac{\alpha_s}{2\pi} \right)^2 \Delta^{(2,Ax)} \right\}. \quad (61)$$

The Born cross section $\sigma_S^{(2,0,\gamma)}$ is given in Eq. (29). We get for the terms $\Delta^{(1,Ve)}$ and $\Delta^{(2,Ve)}$ which arise from the one- and two-loop photon-exchange contributions, respectively:

$$\Delta^{(1,Ve)} = \frac{6\zeta(2)}{\beta} - 8 + \mathcal{O}(\beta), \quad (62)$$

$$\Delta^{(2,Ve)} = C_F \Delta_A^{(2,Ve)} + C_A \Delta_{NA}^{(2,Ve)} + N_f T_R \Delta_L^{(2,Ve)} + T_R \Delta_H^{(2,Ve)}, \quad (63)$$

with

$$\Delta_A^{(2,Ve)} = \frac{12\zeta^2(2)}{\beta^2} - \frac{48\zeta(2)}{\beta} + 24\zeta^2(2) - 4\zeta(2)\left(\frac{35}{3} - 8\ln 2 + 4\ln\beta\right) - 4\zeta(3) + 39 + \mathcal{O}(\beta), \quad (64)$$

$$\Delta_{NA}^{(2,Ve)} = \frac{4\zeta(2)}{\beta}\left(\frac{31}{12} - \frac{11}{2}\ln(2\beta)\right) + 4\zeta(2)\left(\frac{179}{12} - 16\ln 2 - 6\ln\beta\right) - 26\zeta(3) - \frac{151}{9} + \mathcal{O}(\beta), \quad (65)$$

$$\Delta_L^{(2,Ve)} = \frac{4\zeta(2)}{\beta}\left(2\ln(2\beta) - \frac{5}{3}\right) + \frac{44}{9} + \mathcal{O}(\beta), \quad (66)$$

$$\Delta_H^{(2,Ve)} = -\frac{32}{3}\zeta(2) + \frac{176}{9} + \mathcal{O}(\beta^2). \quad (67)$$

In the equations above, $\zeta(2) = \pi^2/6$, $C_A = N_c$, $T_R = 1/2$, and N_f is the number of light quarks, which we take to be massless. For the threshold expansions of the terms $\Delta^{(i,Ax)}$ ($i = 0, 1, 2$), involving Z boson exchange, we find:

$$\Delta^{(0,Ax)} = \frac{s^2}{D_Z} \left\{ \frac{(a_e^Z)^2 + (v_e^Z)^2}{(v_e^\gamma v_Q^\gamma)^2} \left[2(a_Q^Z)^2 \frac{\beta^2}{3 - \beta^2} + (v_Q^Z)^2 \right] + 2 \left(1 - \frac{m_Z^2}{s} \right) \frac{v_e^Z v_Q^Z}{v_e^\gamma v_Q^\gamma} \right\}, \quad (68)$$

$$\Delta^{(1,Ax)} = \mathcal{O}(\beta^2), \quad (69)$$

$$\Delta^{(2,Ax)} = \frac{64\zeta(2)m_Q^4(a_Q^Z)^2 [(v_e^Z)^2 + (a_e^Z)^2]}{(v_Q^\gamma v_e^\gamma)^2(4m_Q^2 - m_Z^2)^2} C_F + \mathcal{O}(\beta), \quad (70)$$

where \hat{v}_f, \hat{a}_f are defined in Eq. (18). While the multiplicative factor $\Delta^{(0,Ax)}$ is given in exact form, the higher order terms are expanded to the appropriate order in β such that the NNLO cross section (61) is obtained to next-to-next-to-leading logarithmic order (NNLL) in β . We observe:

(i) To NNLL in β the NNLO cross section is infrared-finite, i.e., the $Q\bar{Q}$ cross section is equal to the total production cross section to this order. This is due to the fact that close to threshold, real gluon emission is suppressed by a velocity factor with respect to the $Q\bar{Q}$ final state. The two-loop triangle diagrams, studied in [22], do not contribute to the cross section to this order in β .

(ii) In the expansions of $\Delta^{(1,Ve)}$ and $\Delta^{(2,Ve)}$ IR divergences appear at $\mathcal{O}(\beta)$ and $\mathcal{O}(\beta^2)$, respectively. In the expansions of $\Delta^{(1,Ax)}$ and $\Delta^{(2,Ax)}$ such divergences show up to order β^4 and β^3 , respectively.

(iii) The threshold cross section σ_{NNLO} was calculated to NNLL in β in the above energy region, for pure vector exchange, previously in [29] (see also [30]). Putting the axial vector couplings to zero in the above expressions and comparing with [29] we find agreement.

(iv) The first and second-order Z -boson exchange terms $\Delta^{(1,Ax)}$ and $\Delta^{(2,Ax)}$, involving the axial vector coupling \hat{a}_Q , are of order β^2 and β^0 , respectively. $\Delta^{(2,Ax)}$ is thus relevant for an analysis aiming at NNLO accuracy at threshold (counting $\alpha_s \sim \beta$). The analytic result for the axial-vector contribution at $\mathcal{O}(\alpha_s^2)$, which can be obtained to all orders in β from [21, 22], has not been given before in the literature. The term $\Delta^{(2,Ax)}$ is small compared to $\Delta^{(2,Ve)}$, see Fig. 2.

Nevertheless, at a high luminosity linear collider with polarized e^- and e^+ beams one may eventually be able to disentangle the vector and axial-vector induced contributions to the $t\bar{t}$

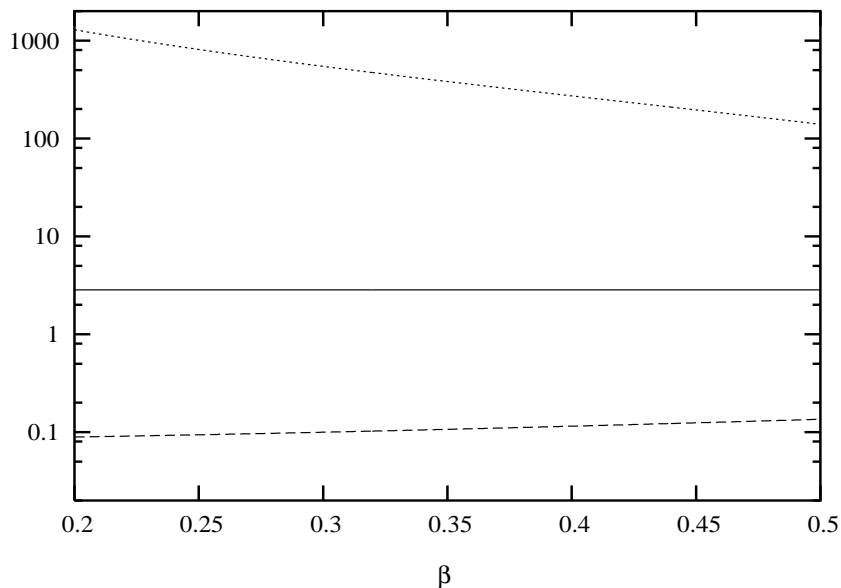


Figure 2: The terms $\Delta^{(2, Ve)}$ (dotted line), $\Delta^{(0, Ax)}$ (dashed line) and $\Delta^{(2, Ax)}$ (solid line), expanded to order β^0 , as functions of β , for the case of $t\bar{t}$ production, using $m_t=172.7$ GeV. $\beta = 0.2$ ($\beta = 0.5$) corresponds to a center-of-mass energy of about 357 GeV (404 GeV).

cross section. A numerical calculation of axial vector contributions in the context of Lippmann-Schwinger equations was performed in [31], and the axial-vector contribution to the threshold cross section at next-to-next-to-leading logarithmic order was determined in [28] by a combination of numerical and analytical calculations.

For completeness we mention that a summation of all terms of the form α_s^n/β^n should be performed when the region of small heavy-quark velocities $\beta \sim \alpha_s$ is approached. The result of the resummation of these leading terms (and of part of the subleading terms) is the well-known Sommerfeld-Sakharov factor (see, for instance [29]). Subleading terms may be resummed by the renormalization group [28] in the context of effective field theory methods. In this paper we are not concerned with these summation methods, as we consider only the region $\beta \gg \alpha_s$.

3.2 Antisymmetric cross section and A_{FB}

Next we perform the threshold expansion of the second-order antisymmetric cross section $\sigma_{NNLO}^{(A)} = \sigma_A^{(2p)}$, given in Eqs. (25) and (38) - (40), in the same manner as was done above for σ_{NNLO} , using the results of [20, 21, 22]. We obtain to NNLL in β :

$$\sigma_{NNLO}^{(A)} = \sigma_A^{(2,0)} \left\{ 1 + C_F \left(\frac{\alpha_s}{2\pi} \right) \Delta^{(A,1)} + C_F \left(\frac{\alpha_s}{2\pi} \right)^2 \Delta^{(A,2)} \right\}, \quad (71)$$

where $\sigma_A^{(2,0)}$ is given in Eq. (38) and

$$\begin{aligned} \Delta^{(A,1)} &= \frac{6\zeta(2)}{\beta} - 6 + \mathcal{O}(\beta), \\ \Delta^{(A,2)} &= C_F \Delta_A^{(A,2)} + C_A \Delta_{NA}^{(A,2)} + N_f T_R \Delta_L^{(A,2)} + T_R (\Delta_H^{(A,2)} + \Delta_{tr}^{(A,2)}), \end{aligned} \quad (72)$$

with

$$\Delta_A^{(A,2)} = \frac{12\zeta^2(2)}{\beta^2} - \frac{36\zeta(2)}{\beta} + 24\zeta^2(2) - 4\zeta(2)\left(\frac{25}{6} - \frac{25}{4}\ln 2 + \frac{9}{2}\ln\beta\right) - \frac{35}{4}\zeta(3) + \frac{70}{3} + \mathcal{O}(\beta), \quad (73)$$

$$\Delta_{NA}^{(A,2)} = \frac{4\zeta(2)}{\beta}\left(\frac{16}{3} - \frac{11}{2}\ln(2\beta)\right) + 4\zeta(2)\left(\frac{67}{6} - \frac{25}{2}\ln 2 - 4\ln\beta\right) - \frac{35}{2}\zeta(3) - 14 + \mathcal{O}(\beta), \quad (74)$$

$$\Delta_L^{(A,2)} = \frac{4\zeta(2)}{\beta}\left(2\ln(2\beta) - \frac{8}{3}\right) + 4 + \mathcal{O}(\beta), \quad (75)$$

$$\Delta_H^{(A,2)} = -\frac{32}{3}\zeta(2) + \frac{56}{3} + \mathcal{O}(\beta^2). \quad (76)$$

The term $\Delta_{tr}^{(A,2)}$ in Eq. (72) is the contribution of the triangle diagrams computed in [22]. It is infrared- and ultraviolet-finite. In the case of $t\bar{t}$ production it is given by

$$\Delta_{tr}^{(A,2)} = \zeta(2)\left(16\ln 2 - \frac{23}{3}\right) - 8\ln 2 + \frac{8}{3}\ln^2 2 + \mathcal{O}(\beta^2). \quad (77)$$

Notice that the the second-order antisymmetric $Q\bar{Q}$ cross section (71) is infrared-finite to NNLL in β and is equal to the total antisymmetric cross section in this order. The terms $\Delta^{(A,1)}$ and $\Delta^{(A,2)}$ become infrared-divergent to order β^2 and β , respectively.

Finally, the second-order forward-backward asymmetry is given near threshold by

$$A_{FB}^{(Q\bar{Q})} = A_{FB,0} C_{FB}, \quad (78)$$

where C_{FB} is the ratio of the curly bracket in Eqs. (71) and of the curly bracket in (61) divided by $(1 + \Delta^{(0,Ax)})$. To NNLL in β it is equal to the complete forward-backward asymmetry A_{FB}^Q .

In Fig. 3 we have plotted the forward-backward asymmetry Eq. (78) to order α_s^2 for $t\bar{t}$ production above threshold in the range $0.2 \leq \beta \leq 0.5$, where C_{FB} is the ratio of two expressions expanded to NNLL in β . The top mass and the other parameters were chosen as given in Eq. (79) below. A comparison with the exact second order asymmetry $A_{FB}^{(t\bar{t})}$ will be made in Section 4.2.

4 Numerical Results

In this section we compute the $Q\bar{Q}$ contributions to A_{FB} to order α_s^2 using the results of Section 2 and the analytic results for the one- and two-loop vector and type A and B axial vector form factors given in [20, 21, 22]. The numerical evaluation of the harmonic polylogarithms that appear in these expressions were made using the code of [34]. For b and c quarks the above formulae are evaluated at and in the vicinity of the Z resonance and for t quarks between $2m_t < \sqrt{s} \leq 1$ TeV. The quark masses, whose values we use are given below, are defined in the on-shell scheme while α_s is the QCD coupling in the $\overline{\text{MS}}$ scheme. When calculating $A_{FB}^{(Q\bar{Q})}$ for b and c quarks around the Z resonance, α_s is defined with respect to the effective $N_f = 5$ flavor theory; that is, the top quark contribution to the gluon self-energy that enters the vector and

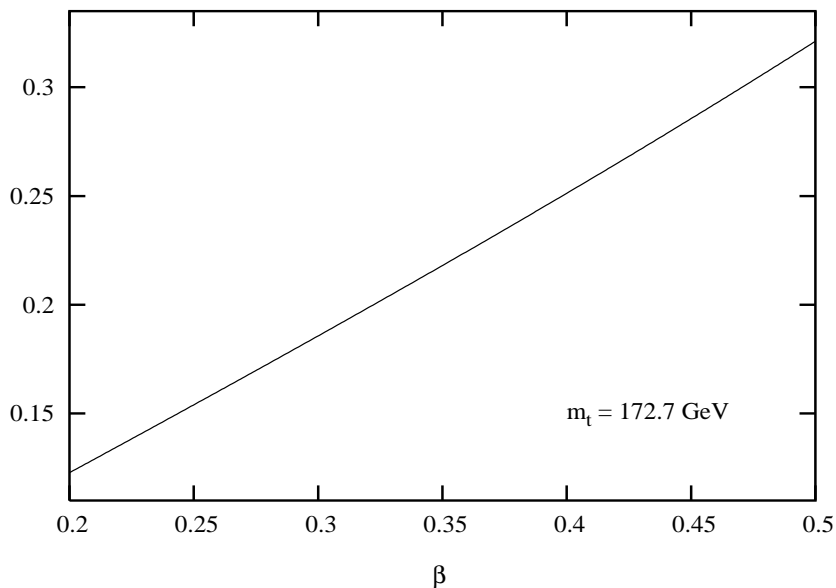


Figure 3: The forward-backward asymmetry $A_{\text{FB}}^{(t\bar{t})}$ to NNLL above the $t\bar{t}$ threshold in the range $0.2 \leq \beta \leq 0.5$ for $\mu = m_t$.

type A axial vector form factors to order α_s^2 is absent. The forward-backward asymmetry for top quarks is computed in the six-flavor theory with the corresponding six-flavor QCD coupling determined from the five-flavor coupling at the matching point $\mu = m_t$. We use the following input values [1]:

$$\begin{aligned}
 m_c &= 1.5 \text{ GeV}, & m_b &= 5 \text{ GeV}, & m_t &= 172.7 \pm 2.9 \text{ GeV}, \\
 m_Z &= 91.1875 \text{ GeV}, & \Gamma_Z &= 2.4952 \text{ GeV}, \\
 \sin^2 \theta_W &= 0.23153, & \alpha_s^{N_f=5}(m_Z) &= 0.1187.
 \end{aligned}
 \tag{79}$$

The value of mass of the top quark is the recent CDF and D0 average [32]. For b and c quarks the type B axial vector contributions are evaluated with the central value of m_t given in (79).

In the following we denote $A_{\text{FB}}^{(Q\bar{Q})}$ evaluated to order α_s and α_s^2 , respectively, by:

$$\begin{aligned}
 A_{\text{FB}}^{(Q\bar{Q})}(\alpha_s) &= A_{\text{FB},0}^{(Q\bar{Q})} \left(1 + A_1^{(Q\bar{Q})} \right), \\
 A_{\text{FB}}^{(Q\bar{Q})}(\alpha_s^2) &= A_{\text{FB},0}^{(Q\bar{Q})} \left(1 + A_1^{(Q\bar{Q})} + A_2^{(Q\bar{Q},A)} + A_2^{(Q\bar{Q},B)} \right).
 \end{aligned}$$

4.1 $A_{\text{FB}}^{(Q\bar{Q})}$ for b and c quarks at and in the vicinity of $\sqrt{s} = m_Z$

Let us first consider the b quark asymmetry. As it is to be computed for $\sqrt{s} \simeq m_Z$ we can safely neglect the masses of the u, d, s , and c quarks which contribute to the second order form factors. (As already mentioned above, the t quark contribution to the gluon self-energy is decoupled.) The type B axial vector form factor $G_1^{(2\ell,B)}$ is non-zero due to the large mass splitting between

	$A_{\text{FB},0}^{(bb)}$	$A_1^{(bb)}$	$A_2^{(bb,A)}$	$A_2^{(bb,B)}$	$A_{\text{FB}}^{(bb)}(\alpha_s)$	$A_{\text{FB}}^{(bb)}(\alpha_s^2)$
$\mu = \frac{m_Z}{2}$	0.103128	-0.000365	-0.000084	0.001147	0.103090	0.103200
$\mu = m_Z$	0.103128	-0.000326	-0.000100	0.000919	0.103094	0.103179
$\mu = 2m_Z$	0.103128	-0.000295	-0.000109	0.000753	0.103097	0.103164

Table 1: The $b\bar{b}$ contributions to A_{FB} for bottom quarks at $\sqrt{s} = m_Z$.

t and b quarks, and to very good approximation one may neglect in these triangle diagram contributions the mass of the b quark. Therefore we use

$$G_1^{(2\ell,B)}(s) = G_1^{(2\ell,B)}(s, m_b = 0, m_b = 0) - G_1^{(2\ell,B)}(s, m_t, m_b = 0), \quad (80)$$

when evaluating Eq. (48), respectively (49), for the b quark. The functions on the right-hand side of (80), whose second and third argument denotes the mass of the quark in the loop and the mass of the external quark, respectively, are given in [33, 22]. (We use the notation of [22].)

Putting $\beta = 1$ in Eq. (49), our result for $A_{\text{FB}}^{(2p,B)}(s = m_Z^2)$ agrees with that of [12].

Table 1 contains the values for the lowest order forward-backward asymmetry at the Z resonance, together with the $b\bar{b}$ contributions to first and second order in α_s for three choices of the renormalization scale μ . The photon and $\gamma - Z$ interference contributions, which are (on the Z resonance) of higher order in the electroweak couplings, are not taken into account. Table 1 shows that the QCD corrections are dominated by the type B contributions: they are about three times as large as the order α_s and about nine times as large as the order α_s^2 corrections. This is due to the fact that we are close to the chiral limit, as $m_b/m_Z \ll 1$. In this limit the order α_s vector and axial vector form factors $F_1^{(1\ell)}$, $G_1^{(1\ell)}$, and the order α_s^2 vector and type A axial vector form factors $F_1^{(2\ell)}$, $G_1^{(2\ell,A)}$ become equal while the chirality-flipping form factors vanish. In this limit $A_1^{(Q\bar{Q})}$ and $A_2^{(Q\bar{Q},A)}$ vanish, too, as an inspection of the above formulae shows. Thus the QCD corrections are dominated by the type B contribution. As it turns out, it amounts to a correction of the lowest order asymmetry by only about one per mille.

In Fig. 4 the first and second order QCD corrections $A_1^{(b\bar{b})}$, $A_2^{(b\bar{b},A)}$, and $A_2^{(b\bar{b},B)}$, evaluated for $\mu = m_Z$, are shown between $88 \text{ GeV} < \sqrt{s} < 95 \text{ GeV}$. Here the contributions from photon exchange are included. Again the QCD corrections are dominated by the type B triangle diagram contributions. Varying the renormalization scale in the range $m_Z/2 \leq \mu \leq 2m_Z$ changes these numbers only by a small amount.

Next we consider the c quark asymmetry for $\sqrt{s} \simeq m_Z$. To very good approximation we can neglect the masses of the c and b quarks in their contribution to the gluon self-energy. Here the type B axial vector form factor $G_1^{(2\ell,B)}$ is again determined by the large mass splitting between t and b quarks. In view of the convention adopted in Eq. (17), where the neutral current couplings of the external quark are factored out, we use now

$$G_1^{(2\ell,B)}(s) = G_1^{(2\ell,B)}(s, m_t, m_c = 0) - G_1^{(2\ell,B)}(s, m_b = 0, m_c = 0) \quad (81)$$

when applying Eq. (48), respectively (49), to the c quark. Again we put $\beta = 1$ in these equations. Eq. (81) is equal in magnitude but opposite in sign to Eq. (80).

Table 2 contains the values for the lowest order c quark forward-backward asymmetry at the Z resonance – without the γ and $\gamma - Z$ contributions –, together with the $c\bar{c}$ contributions to first

	$A_{\text{FB},0}^{(c\bar{c})}$	$A_1^{(c\bar{c})}$	$A_2^{(c\bar{c},A)}$	$A_2^{(c\bar{c},B)}$	$A_{\text{FB}}^{(c\bar{c})}(\alpha_s)$	$A_{\text{FB}}^{(c\bar{c})}(\alpha_s^2)$
$\mu = \frac{m_Z}{2}$	0.073592	-0.000170	-0.000060	-0.002418	0.073580	0.073397
$\mu = m_Z$	0.073592	-0.000152	-0.000063	-0.001938	0.073581	0.073434
$\mu = 2m_Z$	0.073592	-0.000138	-0.000064	-0.001586	0.073582	0.073460

Table 2: The $c\bar{c}$ contributions to A_{FB} for charm quarks at $\sqrt{s} = m_Z$.

and second order in α_s for three choices of the renormalization scale μ . The QCD corrections are dominated again by the type B term, which in this case is about two per mille of the leading order asymmetry. The increase by a factor of about two as compared to the b quark results from the fact that $|v_c^Z| < |v_b^Z|$, c.f. Eq. (49).

In Fig. 5 the first and second order QCD corrections $A_1^{(c\bar{c})}$, $A_2^{(c\bar{c},A)}$, and $A_2^{(c\bar{c},B)}$, evaluated for $\mu = m_Z$, are shown between $88 \text{ GeV} < \sqrt{s} < 95 \text{ GeV}$, including the contributions from photon exchange. For c quarks, too, the QCD corrections are dominated by the type B triangle diagram contributions.

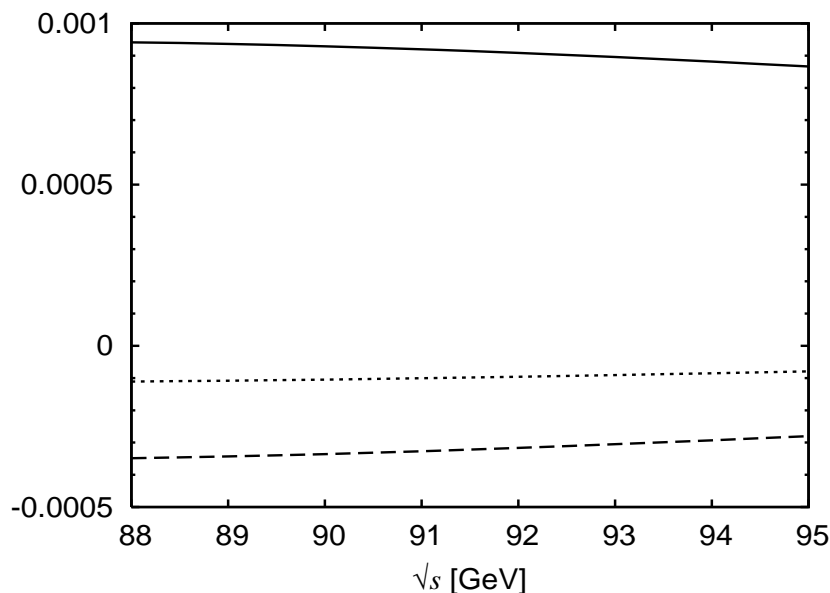


Figure 4: First and second order QCD corrections $A_1^{(b\bar{b})}$ (dashed), $A_2^{(b\bar{b},A)}$ (dotted), and $A_2^{(b\bar{b},B)}$ (solid) for $\mu = m_Z$ in the vicinity of the Z resonance.

In Fig. 6 the $b\bar{b}$ and $c\bar{c}$ forward-backward asymmetries to order α_s^2 , $A_{\text{FB}}^{(b\bar{b})}(\alpha_s^2)$ and $A_{\text{FB}}^{(c\bar{c})}(\alpha_s^2)$ are displayed between $88 \text{ GeV} < \sqrt{s} < 95 \text{ GeV}$, using $\mu = m_Z$. Figs. 4, 5 show that the order α_s^2 asymmetry is increased, in the case of b quarks, by about one per mille and decreased, in the case of c quarks, by about two per mille of the respective lowest order asymmetry in the whole energy range considered. Varying the renormalization scale in the range $m_Z/2 \leq \mu \leq 2m_Z$ changes the asymmetries shown in Fig. 6 only by a very small amount.

The complete forward-backward asymmetry to order α_s^2 for b and c quarks at and in the vicinity of the Z resonance is dominated by the respective three- and four-parton contributions.

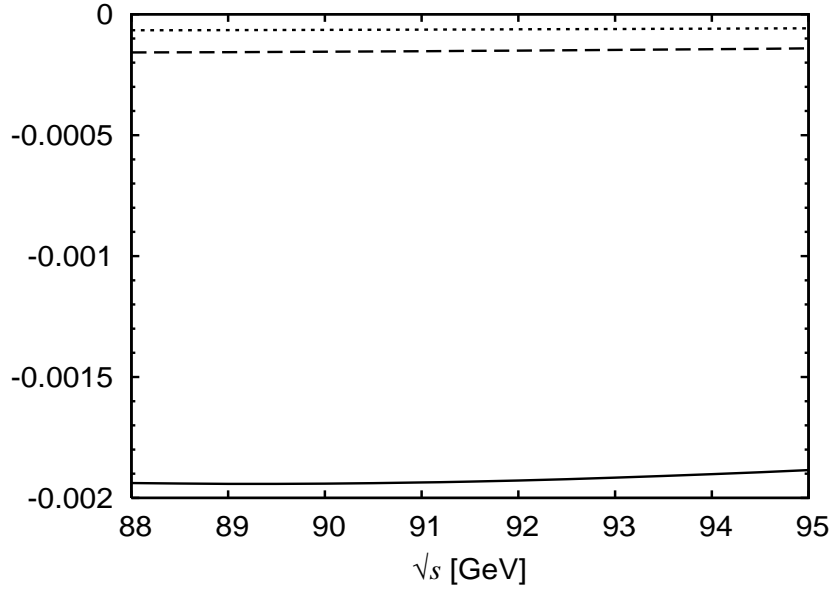


Figure 5: First and second order QCD corrections $A_1^{(c\bar{c})}$ (dashed), $A_2^{(c\bar{c},A)}$ (dotted), and $A_2^{(c\bar{c},B)}$ (solid) for $\mu = m_Z$ in the vicinity of the Z resonance.

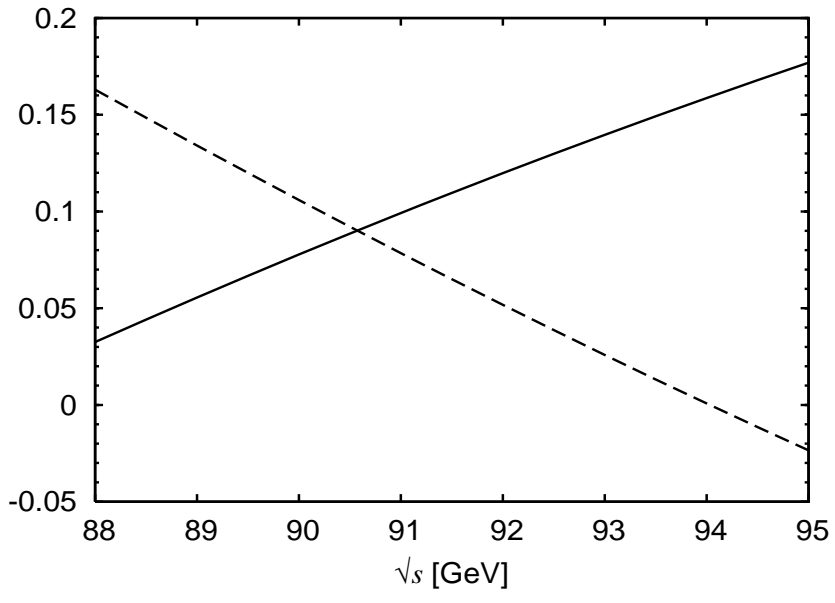


Figure 6: $A_{\text{FB}}^{(bb)}(\alpha_s^2)$ (solid) and $A_{\text{FB}}^{(c\bar{c})}(\alpha_s^2)$ (dashed) for $\mu = m_Z$ in the vicinity of the Z resonance.

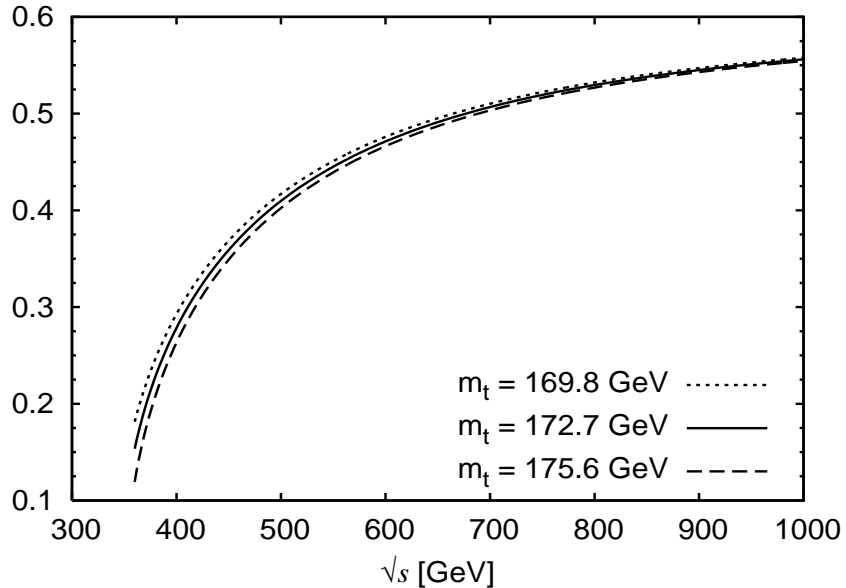


Figure 7: Leading order asymmetry $A_{\text{FB},0}^{(t\bar{t})}$ for three values of the top quark mass.

A complete computation of these terms to order α_s^2 has not yet been done for $m_b, m_c \neq 0$. Nevertheless, we expect that the respective results of [14], which were obtained in the massless limit, will not change dramatically.

4.2 $A_{\text{FB}}^{(t\bar{t})}$ for top quarks above threshold

Finally we compute the $t\bar{t}$ contributions to the forward-backward asymmetry in the reaction $e^+e^- \rightarrow t\bar{t}X$, sufficiently far away from the pair production threshold in order that perturbation theory in α_s is applicable. That is, the following results apply to events with t and \bar{t} velocities $\beta \gg \alpha_s$. As already stated above, α_s is defined in the six flavor QCD, with all quarks but the top quark taken to be massless. The value of $\alpha_s(\mu = m_t)$ is determined from the input value (79), and values of α_s at other energy scales are obtained by two-loop renormalization group evolution. Most of the results below are presented for three values of the top quark mass: the present central and 1 s.d. upper and lower values 172.7 GeV, 175.6 GeV, and 169.8 GeV, respectively. The type B contribution to $A_{\text{FB}}^{(t\bar{t})}$, Eq. (48), is computed with the two-loop axial vector form factor

$$G_1^{(2\ell,B)}(s) = G_1^{(2\ell,B)}(s, m_t, m_t) - G_1^{(2\ell,B)}(s, m_b = 0, m_t). \quad (82)$$

which is given in [22].

In the following we consider the energy range $360 \text{ GeV} \leq \sqrt{s} \leq 1 \text{ TeV}$. In Fig. 7 the leading order asymmetry $A_{\text{FB},0}^{(t\bar{t})}$ is shown for three values of the top quark mass. In Figs. 8 and 9 the order α_s correction $A_1^{(t\bar{t})}$ is displayed for three values of the renormalization scale μ and fixed top quark mass, and for three values of m_t and fixed μ , respectively. The analogous cases are shown in Figs. 10 and 11 for the order α_s^2 correction $A_2^{(t\bar{t},A)}$. The triangle diagram contributions

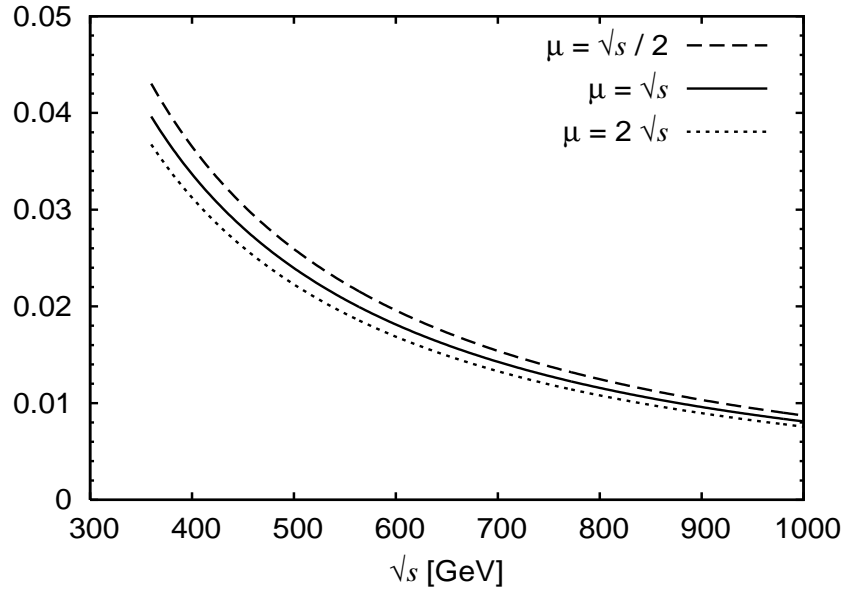


Figure 8: Order α_s correction $A_1^{(t\bar{t})}$ for three values of the renormalization scale μ , using $m_t = 172.7$ GeV.

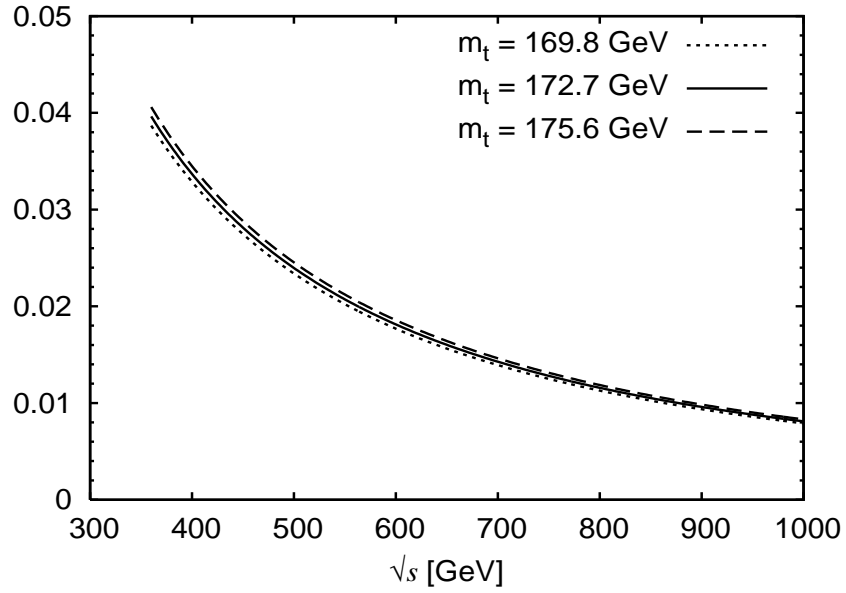


Figure 9: Order α_s correction $A_1^{(t\bar{t})}$ for three values of the top quark mass, using $\mu = \sqrt{s}$.

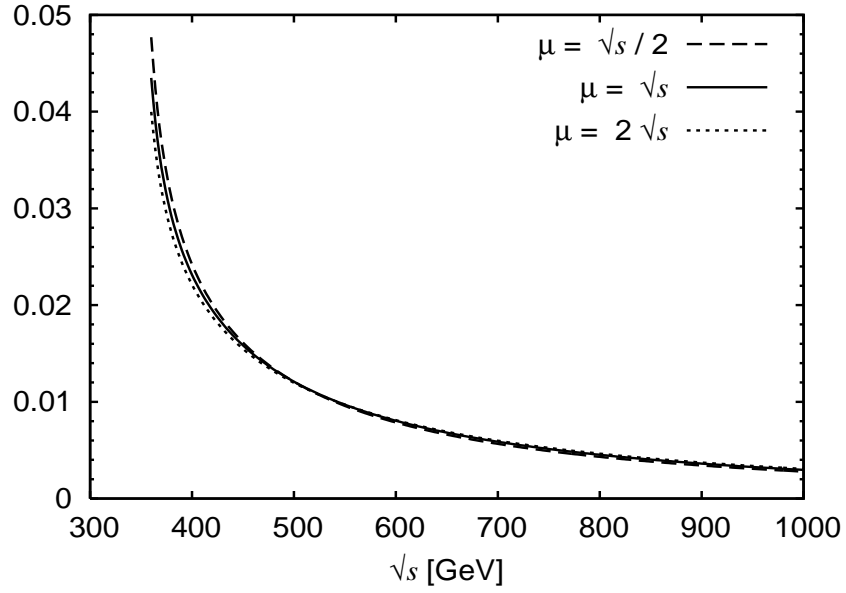


Figure 10: Order α_s^2 correction $A_2^{(t\bar{t},A)}$ for three values of the renormalization scale μ , using $m_t = 172.7$ GeV.

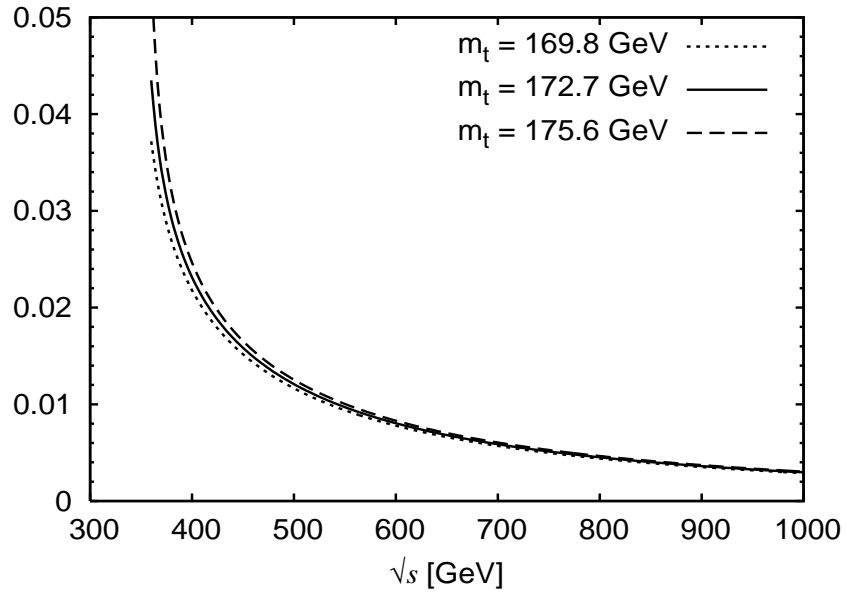


Figure 11: Order α_s^2 correction $A_2^{(t\bar{t},A)}$ for three values of the top quark mass, using $\mu = \sqrt{s}$.

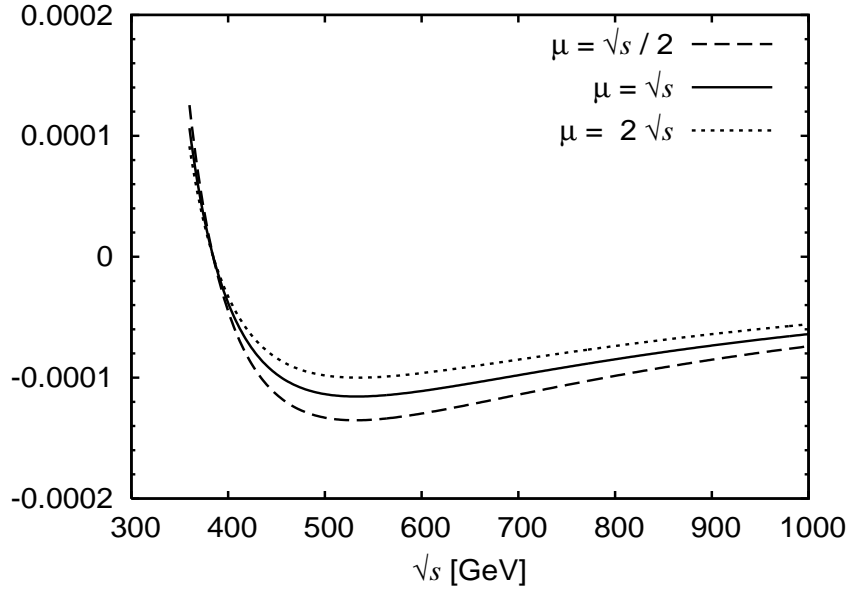


Figure 12: Order α_s^2 correction $A_2^{(t\bar{t}, B)}$ for three values of the renormalization scale μ , using $m_t = 172.7$ GeV.

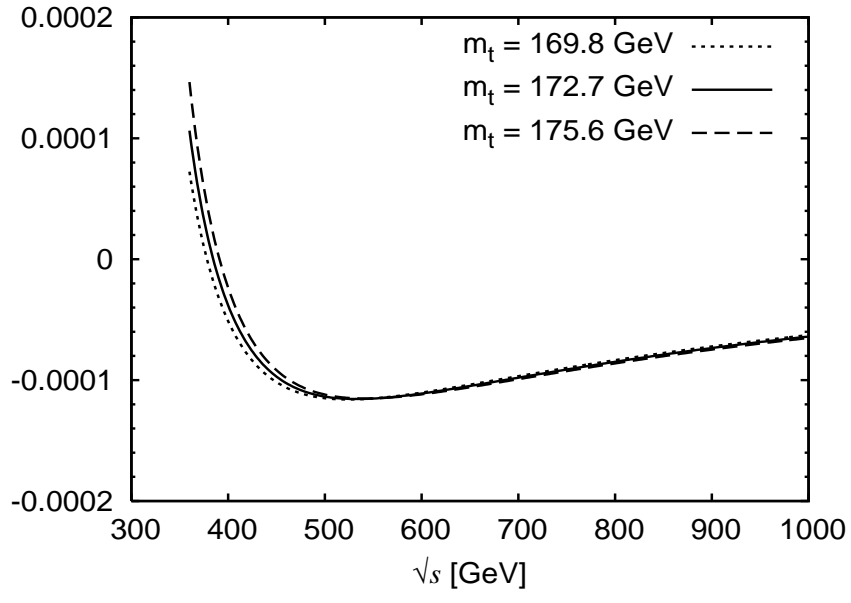


Figure 13: Order α_s^2 correction $A_2^{(t\bar{t}, B)}$ for three values of the top quark mass, using $\mu = \sqrt{s}$.

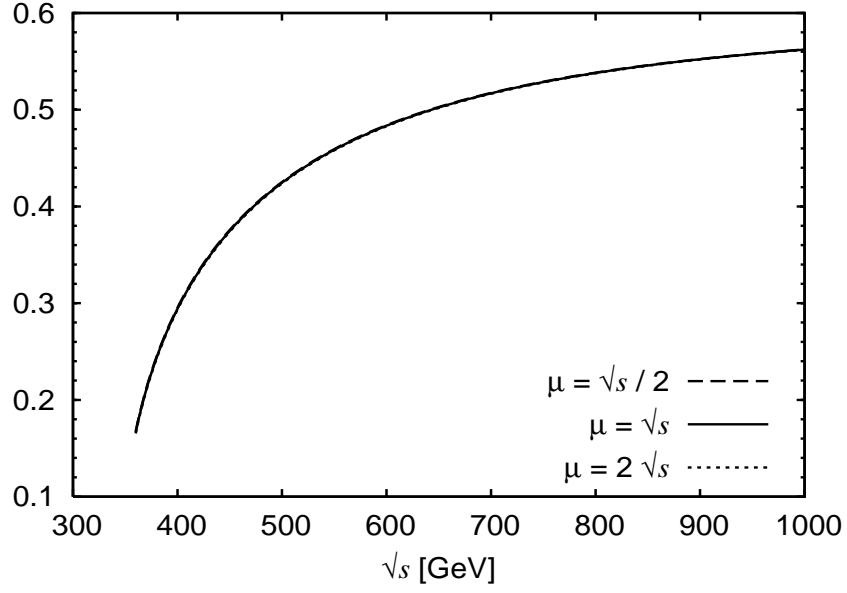


Figure 14: Forward-backward asymmetry $A_{\text{FB}}^{(t\bar{t})}(\alpha_s^2)$ for three values of the renormalization scale μ , using $m_t = 172.7$ GeV.

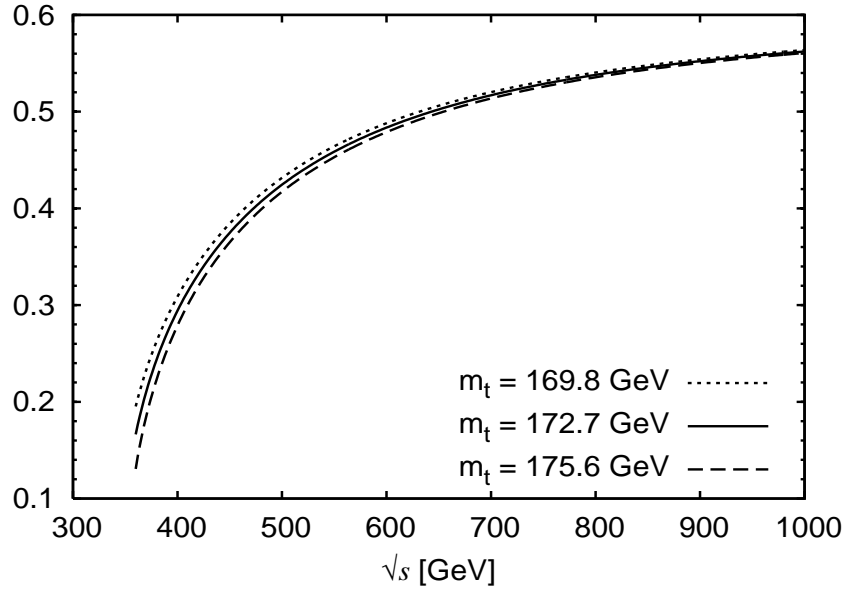


Figure 15: Forward-backward asymmetry $A_{\text{FB}}^{(t\bar{t})}(\alpha_s^2)$ for three values of the top quark mass, using $\mu = \sqrt{s}$.

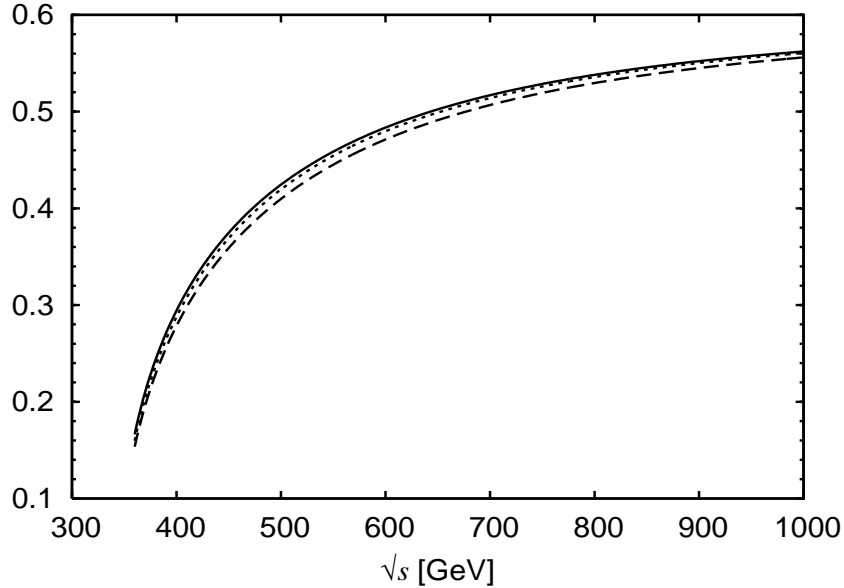


Figure 16: Forward-backward asymmetry to lowest, first and second order in α_s using $m_t = 172.7$ GeV and $\mu = \sqrt{s}$. $A_{\text{FB},0}^{(t\bar{t})}$ (dashed), $A_{\text{FB}}^{(t\bar{t})}(\alpha_s)$ (dotted), $A_{\text{FB}}^{(t\bar{t})}(\alpha_s^2)$ (solid).

$A_2^{(t\bar{t},B)}$ are given in Fig. 12 and Fig. 13 for three values of μ and m_t , respectively. From these figures we conclude that the two-parton QCD corrections to the lowest order asymmetry are moderate to small for $\sqrt{s} \geq 400$ GeV. At $\sqrt{s} = 400$ GeV, $A_1^{(t\bar{t})}$ is about 3.3 percent while $A_2^{(t\bar{t},A)}$ is about 2.4 percent. As expected, the relative importance of the order α_s^2 corrections increases as the centre-of-mass energy approaches the threshold region: for $\sqrt{s} \simeq 360$ GeV, $A_2^{(t\bar{t},A)}$ is larger than $A_1^{(t\bar{t})}$, signaling that perturbation theory in α_s is no longer applicable. Contrary to the case of b and c quarks at the Z resonance the two-loop type B contributions are two orders of magnitude smaller than $A_2^{(t\bar{t},A)}$.

Figs. 14 and 15 show the forward-backward asymmetry $A_{\text{FB}}^{(t\bar{t})}(\alpha_s^2)$ for three values of the renormalization scale and three values of the top quark mass, respectively. The dependence of the second order asymmetry on μ is small: changing μ from $\sqrt{s}/2$ to $2\sqrt{s}$ changes $A_{\text{FB}}^{(t\bar{t})}(\alpha_s^2)$, for fixed m_t , only by about 1 percent at $\sqrt{s} \gtrsim 360$ GeV, and this dependence on μ decreases with increasing c. m. energy.

In Fig. 16 the $t\bar{t}$ asymmetry is displayed to lowest, first, and second order in α_s . This figure shows that for c. m. energies sufficiently away from threshold the QCD corrections are under control.

Finally, a comparison is made in Fig. 17 between the exact second order forward-backward asymmetry $A_{\text{FB}}^{(t\bar{t})}(\alpha_s^2)$ as given in Fig. 16 and the values obtained from the near-threshold NNLL formula Eq. (78). For $\sqrt{s} \lesssim 360$ GeV corresponding to $\beta \lesssim 0.3$ the deviation of the NNLL from the respective exact value is less than 5 percent.

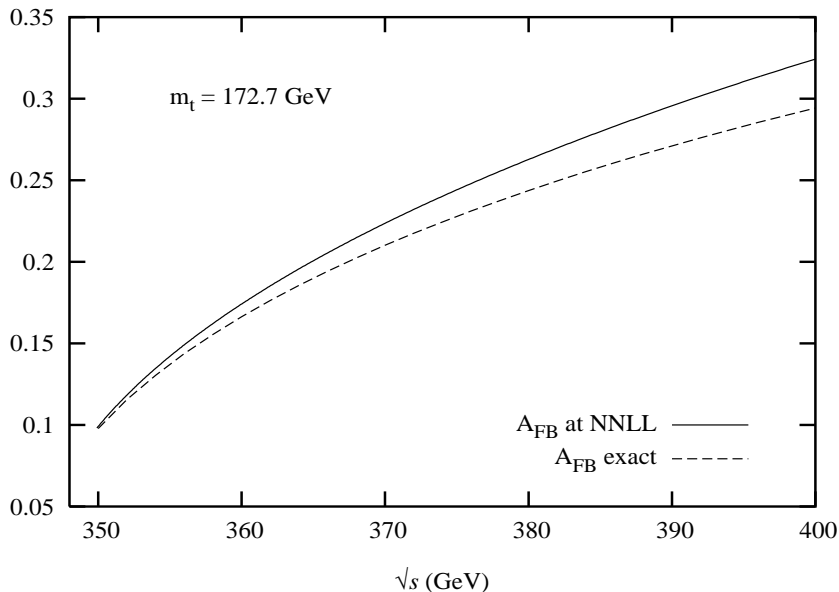


Figure 17: The second order forward-backward asymmetry $A_{\text{FB}}^{(t\bar{t})}(\alpha_s^2)$ near threshold: exact values (dashed) as given in Fig. 16 and the values obtained from the near-threshold formula Eq. (78) (solid), using $\mu = m_t = 172.7$ GeV.

5 Summary and Outlook

Future experiments on heavy-quark production at a planned linear e^+e^- collider aim at very precise measurements of the neutral-current couplings of these quarks. An important observable for this purposes is the forward-backward asymmetry A_{FB}^Q in inclusive heavy quark production, $e^+e^- \rightarrow \gamma^*, Z^* \rightarrow Q + X$. The projected accuracies with which A_{FB}^Q can be measured in future b or t quark production requires also the precise determination of these observables within the Standard Model. In particular, a computation of the order α_s^2 QCD contributions to A_{FB}^Q for massive quarks is mandatory.

In view of these perspectives we have calculated the contribution of the $Q\bar{Q}$ final state to A_{FB}^Q in NNLO QCD. As discussed above, and explicitly shown for the $Q\bar{Q}$ final state, the contributions of the two-parton and of the three- plus four-parton states to the second-order forward-backward asymmetry are separately infrared-finite. We have provided formulae for the symmetric and antisymmetric $Q\bar{Q}$ cross sections σ_S and σ_A which yield $A_{\text{FB}}^{(Q\bar{Q})}$. These formulae hold for any center-of-mass energy. Specifically, in the energy region near threshold where the quark velocity β satisfies $\alpha_s \ll \beta \ll 1$, we have expanded the order α_s and α_s^2 QCD corrections to σ_S and σ_A to NNLL in β . To this order in β the $Q\bar{Q}$ cross sections are equal to the corresponding total cross sections. Therefore, an (analytic) expression is obtained for the forward-backward asymmetry A_{FB}^Q to order α_s^2 and order β near threshold.

Moreover, we have computed the two-parton forward-backward asymmetry $A_{\text{FB}}^{(Q\bar{Q})}$ for b and c quarks on and near the Z -boson resonance and for t quarks for center-of-mass energies \sqrt{s} above threshold to 1 TeV. The two-parton asymmetry is determined by the heavy-quark vector and axial vector form factors. To order α_s^2 the axial vector form factors receive besides type

A (universal) corrections also triangle diagram contributions resulting from the large mass splitting between t and b quarks. These triangle diagram terms dominate, for $\sqrt{s} \sim m_Z$, the QCD corrections from the $Q\bar{Q}$ final state to A_{FB}^b and A_{FB}^c . This is due to the fact that here one is close to the chiral limit. However, the complete order α_s^2 QCD corrections to these asymmetries are dominated by the contributions from the three- and four-parton final states, which were calculated so far only for massless quarks [14]. For top quarks the triangle diagram contributions to A_{FB}^t are negligible compared to the type A corrections. These corrections from the $t\bar{t}$ final state to the lowest order asymmetry are moderate for large \sqrt{s} and increase in size towards threshold. The order α_s^2 corrections are important, as the analysis in Section 4.2 shows.

We plan to determine in the near future also the contribution of the three- and four parton-final states to the order α_s^2 forward-backward asymmetry for massive quarks.

Acknowledgment

This work was supported by Deutsche Forschungsgemeinschaft (DFG), SFB/TR9, by DFG-Graduiertenkolleg RWTH Aachen, by the Swiss National Science Foundation (SNF) under contract 200020-109162, by the European Union under the contract HPRN-CT2002-00311 (EURIDICE), by a European Commission Marie Curie Fellowship under contract number MEIF-CT-2006-024178, by MCYT (Spain) under Grant FPA2004-00996, by Generalitat Valenciana (Grants GRUPOS03/013 and GV05/015), and by the USA DoE under the grant DE-FG03-91ER40662, Task J.

References

- [1] [LEP and SLD Collaborations], “Precision electroweak measurements on the Z resonance,” hep-ex/0509008.
- [2] D. Abbaneo *et al.* [LEP Heavy Flavor Working Group], Eur. Phys. J. C **4** (1998) 185. LEP/SLD heavy flavour working group, “Final Input Parameters for the LEP/SLD Heavy Flavour Analyses”, LEPHF/2001-01; <http://lepewwg.web.cern.ch/LEPEWWG/heavy/>
- [3] J. A. Aguilar-Saavedra *et al.* [ECFA/DESY LC Physics Working Group Collaboration], “TESLA Technical Design Report Part III: Physics at an e^+e^- Linear Collider”, DESY-report 2001-011 (hep-ph/0106315).
- [4] R. Hawkins and K. Mönig, Eur. Phys. J. direct C **1** (1999) 8 [hep-ex/9910022].
- [5] J. Erler, S. Heinemeyer, W. Hollik, G. Weiglein and P. M. Zerwas, Phys. Lett. B **486** (2000) 125 [hep-ph/0005024].
- [6] M. Böhm *et al.*, “Forward - Backward Asymmetries,” in: CERN Yellow Report “Z Physics at LEP 1”, CERN 89-08 (1989), G. Altarelli *et al.* (eds.).
- [7] D. Y. Bardin, P. Christova, M. Jack, L. Kalinovskaya, A. Olchevski, S. Riemann and T. Riemann, Comput. Phys. Commun. **133** (2001) 229 [hep-ph/9908433].
- [8] A. Freitas and K. Mönig, Eur. Phys. J. C **40** (2005) 493 [hep-ph/0411304].
- [9] J. Jersak, E. Laermann and P. M. Zerwas, Phys. Rev. D **25** (1982) 1218 [Erratum-ibid. D **36** (1987) 310].

- [10] B. Arbuzov, D. Y. Bardin and A. Leike, *Mod. Phys. Lett. A* **7** (1992) 2029 [Erratum-ibid. *A* **9** (1994) 1515].
- [11] A. Djouadi, B. Lampe and P. M. Zerwas, *Z. Phys.* **C67** (1995) 123 [[hep-ph/9411386](#)].
- [12] G. Altarelli and B. Lampe, *Nucl. Phys.* **B391** (1993) 3.
- [13] V. Ravindran and W. L. van Neerven, *Phys. Lett.* **B445** (1998) 214. [[hep-ph/9809411](#)].
- [14] S. Catani and M.H. Seymour, *JHEP* **07** (1999) 023 [[hep-ph/9905424](#)].
- [15] W. Bernreuther, A. Brandenburg and P. Uwer, *Phys. Rev. Lett.* **79** (1997) 189 [[hep-ph/9703305](#)]; A. Brandenburg and P. Uwer, *Nucl. Phys.* **B515** (1998) 279 [[hep-ph/9708350](#)].
- [16] G. Rodrigo, A. Santamaria and M. S. Bilenky, *Phys. Rev. Lett.* **79** (1997) 193 [[hep-ph/9703358](#)]; *Nucl. Phys.* **B554** (1999) 257 [[hep-ph/9905276](#)].
- [17] P. Nason and C. Oleari, *Phys. Lett. B* **407** (1997) 57 [[hep-ph/9705295](#)]; *Nucl. Phys.* **B521** (1998) 237, [[hep-ph/9709360](#)].
- [18] W. Bernreuther, A. Brandenburg and P. Uwer, [hep-ph/0008291](#).
- [19] A. Gehrmann-De Ridder, T. Gehrmann and E. W. N. Glover, *JHEP* **0509** (2005) 056 [[hep-ph/0505111](#)].
- [20] W. Bernreuther, R. Bonciani, T. Gehrmann, R. Heinesch, T. Leineweber, P. Mastrolia and E. Remiddi, *Nucl. Phys. B* **706**, 245 (2005) [[hep-ph/0406046](#)].
- [21] W. Bernreuther, R. Bonciani, T. Gehrmann, R. Heinesch, T. Leineweber, P. Mastrolia and E. Remiddi, *Nucl. Phys. B* **712** (2005) 229 [[hep-ph/0412259](#)].
- [22] W. Bernreuther, R. Bonciani, T. Gehrmann, R. Heinesch, T. Leineweber and E. Remiddi, *Nucl. Phys. B* **723** (2005) 91 [[hep-ph/0504190](#)].
- [23] S. Catani, *Phys. Lett. B* **427** (1998) 161 [[hep-ph/9802439](#)].
- [24] G. Sterman and M. E. Tejeda-Yeomans, *Phys. Lett. B* **552** (2003) 48 [[hep-ph/0210130](#)].
- [25] D. R. Yennie, S. C. Frautschi and H. Suura, *Annals Phys.* **13** (1961) 379.
- [26] S. Catani, S. Dittmaier and Z. Trocsanyi, *Phys. Lett. B* **500** (2001) 149 [[hep-ph/0011222](#)].
- [27] M. Beneke, A. Signer and V. A. Smirnov, *Phys. Lett. B* **454** (1999) 137 [[hep-ph/9903260](#)].
- [28] A. H. Hoang, A. V. Manohar, I. W. Stewart and T. Teubner, *Phys. Rev. D* **65** (2002) 014014 [[hep-ph/0107144](#)].
- [29] A. Czarnecki and K. Melnikov, *Phys. Rev. Lett.* **80** (1998) 2531 [[hep-ph/9712222](#)].
- [30] A. H. Hoang, *Phys. Rev. D* **56** (1997) 7276 [[hep-ph/9703404](#)].
- [31] J. H. Kühn and T. Teubner, *Eur. Phys. J. C* **9** (1999) 221 [[hep-ph/9903322](#)].
- [32] The Tevatron Electroweak Working Group, J.F. Arguin et al., “Combination of CDF and D0 results on the top-quark mass,” [hep-ex/0507091](#).
- [33] B. A. Kniehl and J. H. Kühn, *Nucl. Phys. B* **329**, 547 (1990).
- [34] T. Gehrmann and E. Remiddi, *Comput. Phys. Commun.* **141** (2001) 296 [[hep-ph/0107173](#)]; D. Maître, *Comput. Phys. Commun.* **174** (2006) 222 [[hep-ph/0507152](#)].